Check for updates

Recent progress in multifunctional theranostic hydrogels: the cornerstone of next-generation wound care technologies

Laxmanan Karthikeyan[a,b] and Hyun Wook Kang [ID] *[b,c]

Theranostic hydrogels represent a groundbreaking approach by integrating therapeutic and diagnostic capabilities within a single platform, enabling real-time monitoring of wounds and precise treatment applications. These advanced materials are engineered to maintain a moist, antimicrobial environment while promoting tissue regeneration through enhanced conductivity and bioactivity. Theranostic hydrogels, which incorporate electro-responsive and stimuli-sensitive polymers, enable the continuous monitoring of important biomarkers like pH and glucose levels, ensuring accurate, timely therapeutic interventions. Bioelectronic components, including flexible biosensors, wearable electronic patches, and implantable microdevices, significantly enhance the functionality of wound care technology. Recent advancements in materials science have further improved the adaptability of these hydrogels, allowing for the integration of nanomaterials to accelerate healing and optimize therapeutic outcomes. Additionally, these hydrogels can be combined with cutting-edge technologies such as 3D bioprinting and artificial intelligence, paving the way for personalized wound care solutions tailored to individual patient needs. This review highlights recent progress in theranostic hydrogels and their transformative potential in managing complex wounds. By integrating both diagnostics and therapeutic capabilities into a multifunctional platform, theranostic hydrogels represent a promising frontier for next-generation wound care technologies.

1. Introduction

Theranostics represents a groundbreaking approach for modern medicine, seamlessly integrating therapeutic and diagnostic capabilities to enable simultaneous treatment and real-time monitoring of medical conditions. First conceptualized by Funkhouser in 1998, this innovative strategy has revolutionized the way diseases are managed by providing a dual-function platform that enhances precision and efficacy of clinical interventions. The roots of theranostics can be traced back to the 1940s, with the pioneering use of radioactive iodine, which plays a dual role in both diagnosing and treating thyroid cancer. This early application laid the groundwork for the fundamental principles that continue to drive advancements in theranostic technologies today.[1–3] Precision medicine is a healthcare strategy designed to improve treatment effec-

tiveness by customizing medical procedures to an individual's distinct and dynamic health profile. Precision medicine utilizes data by integrating disciplines such as drug delivery, statistical analysis, and genetics to enable individualized, informed care. This technique uses real-time patient data to feed decision-making algorithms for drug selection, dose adjustments, and treatment scheduling. This tailored approach guarantees that patients have appropriate therapy at the optimal moment, resulting in enhanced outcomes relative to traditional, uniform treatment methods.[4,5]

Wearable theranostic devices, such as smartwatches and mobile health monitors, have emerged as transformative tools in the field of precision medicine. These advanced systems offer non-invasive, user-friendly solutions for continuous and accurate monitoring of various health parameters. By leveraging cutting-edge sensors and real-time data analysis, wearable devices enable early detection of abnormalities, personalized health management, and timely medical interventions.[6–8] A primary benefit of these devices is their ability to integrate predictive analytics, allowing healthcare providers and patients to make informed decisions based on continuous health data. For instance, wearable monitors can track vital signs, activity levels, or biochemical markers, providing insights into a patient's condition without the need for frequent hospital visits. This not only reduces the burden on traditional health-

[a]*Industry–University Cooperation Foundation, Pukyong National University, Busan 48513, Republic of Korea*

[b]*Center for Marine Integrated Bionics Technology, The National Key Research Institutes in Universities, Pukyong National University, Busan 48513, Republic of Korea*

[c]*Major of Biomedical Engineering, Division of Smart Healthcare, College of Information Technology and Convergence, Pukyong National University, Busan 48513, Republic of Korea. E-mail: wkang@pukyong.ac.kr*

care systems but also minimizes the inconvenience and stress often associated with lengthy treatment processes.[9] Furthermore, wearable theranostic devices bridge the gap between patients and healthcare professionals, enabling remote monitoring and tailored treatment adjustments. These innovations address critical challenges in conventional healthcare, such as delayed diagnosis, inefficient resource allocation, and limited accessibility. As a result, they significantly enhance the efficiency, accuracy, and personalization of medical care, ensuring patients receive timely and appropriate treatment for improved outcomes.[10,11]

Since Wichterle *et al.*'s groundbreaking use of hydrated hydroxymethyl methacrylate (HEMA) networks in contact lenses during the 1960s, a wide range of functional hydrogels have garnered substantial research attention for their potential applications in tissue engineering and biomedicine.[12,13] Hydrogels are hydrophilic polymers with a three-dimensional (3D) network framework capable of absorbing and holding large amounts of water. Over the past decade, they have been extensively utilized in ocular drug delivery and wound healing, with various products, such as ReSure® and DEXTENZA®, already available on the market.[14,15] Hydrogels play a crucial role in biomedical applications, particularly in wound healing.[16] The use of hydrogels in cancer therapy is rapidly expanding due to their potential for tumor eradication.[17] Beyond advancing cancer immunotherapy and vaccine development, hydrogels also hold promise in photothermal therapy (PTT) and targeted drug delivery. Stimuli-responsive hydrogels, reacting to near-infrared (NIR) light or pH changes, show great promise for precise and effective cancer treatment.[18]

This review explores the innovative application of theranostic hydrogels as integrated platforms for multifunctional wound care devices, with a particular emphasis on their role in sustained and responsive drug delivery to improve therapeutic outcomes. We focus on the ability of these hydrogels to deliver bioactive agents in a controlled manner while adapting to the complex and often hostile wound microenvironment. Particular attention is paid to functionalized hydrogels endowed with antimicrobial, anti-inflammatory, and immune-regulatory properties, which, when combined with engineered materials, present a transformative strategy to overcome the limitations of conventional wound dressings. While existing reviews have largely addressed either the chemical composition of hydrogels or their therapeutic functions separately, this work uniquely integrates recent progress in multifunctional theranostic hydrogels, emphasizing platforms that enable both treatment and real-time monitoring. We further advance the discourse by highlighting cutting-edge developments such as biosensor-embedded systems, bioresponsive behaviors, and the integration of artificial intelligence (AI) to enhance precision wound care. By offering a structure–function perspective and translational outlook, this review provides a comprehensive and forward-looking framework to guide the rational design of next-generation theranostic hydrogels. Our objective is to inspire novel design strategies and accelerate progress in the clinical translation of intelligent hydrogel-based wound care technologies (Scheme 1).

2. Overview of hydrogels and the wound microenvironment

Hydrogels are the most versatile three-dimensional polymer networks, which can absorb and hence retain greater amounts of water. Their unique properties have led to advancements in various sectors, including biomedicine, environmental appli-
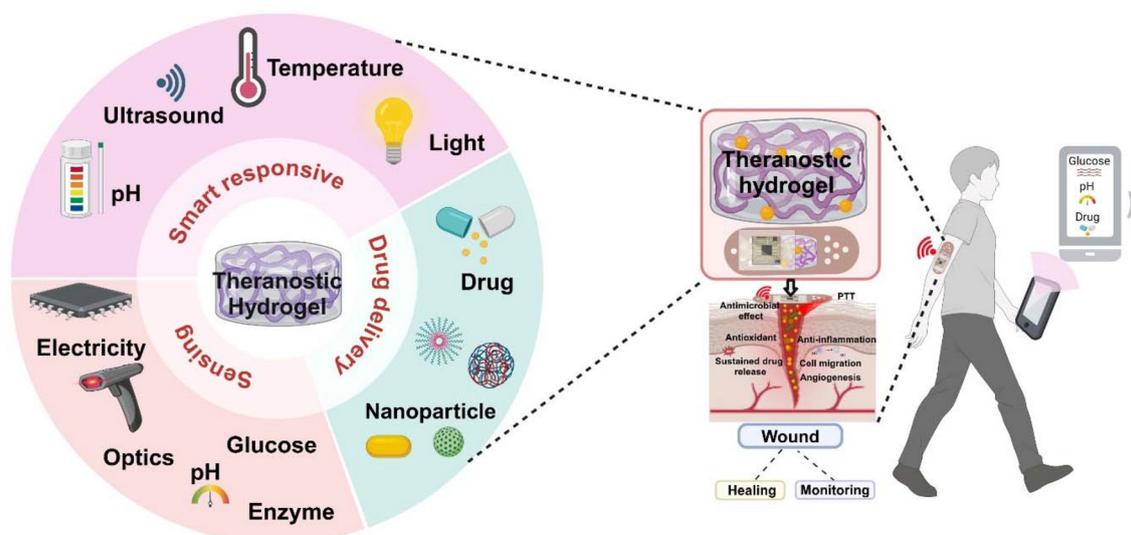
Scheme 1 Schematic illustration of a theranostic hydrogel for wound healing and real-time monitoring. This smart, responsive hydrogel integrates therapeutic and diagnostic functionalities, enabling controlled drug delivery, real-time sensing of the wound microenvironment, and adaptive healing responses for enhanced wound care.

cations, and industrial processes. Recent developments have also integrated artificial intelligence (AI) technology, enabling smarter development and expansion of hydrogel properties for major areas like drug delivery and wound healing.[19–22] The features and performance of hydrogels are primarily determined by chemical structure. These materials may be fabricated with either polymers derived naturally or synthetically. Synthetic hydrogels are often synthesized from monomers such as acrylamide or acrylic acid by various polymerization methods including UV-induced polymerization, free radical polymerization or crosslinking. Conversely, natural hydrogels are derived from proteins and polysaccharides, as a result of physical or chemical crosslinking methods.[23–25]

The characteristics obtained after synthesis are primarily governed by the chemistry of the polymers utilized. Properties like swelling behavior, mechanical strength, and biocompatibility are shaped by functional entities present on the surface of the polymer, such as carboxyl, amine and hydroxyl groups. Groups with carboxyl ends enhance the hydrogel's hydrophilicity, improving its capacity to absorb and retain water. On the other hand, amine groups facilitate interactions with biological molecules, which can be essential for tissue regeneration and the delivery of various drugs. Surface functionalization tends to play an important role in the customization of hydrogels for specific biomedical applications. Accordingly, the stringent design of polymer chemistry is also essential for optimizing their performance for various uses.[26,27] The extent of crosslinking is also a crucial element for deciding the core features of hydrogels. Hydrogels with a high degree of crosslinking tend to be more rigid and absorb less water, while those with lower crosslinking levels have better water retention capabilities. The chemical structure of hydrogels also governs their sensitivity towards influential factors like pH, light and temperature. Research advancements in hydrogel chemistry have led to the emergence of "smart" hydrogels. These hydrogels are fabricated in such a way that they respond to changing environmental factors. Moreover, the chemical composition impacts the biodegradability and biocompatibility of hydrogels, making them proficient candidates for various biomedical streams. The development of hydrogels is done by carefully considering these aspects to obtain tailored hydrogels. Current research focuses on enhancing these attributes by incorporating natural materials like collagen, chitosan, and hyaluronic acid into hydrogel synthesis.[28–31]

2.1. Crosslinking mechanisms for hydrogels

The mechanistic action of crosslinking hydrogels involves the development of chemical or physical bonds between polymer chains, which enhances the material's stability and mechanical properties. These crosslinks may be induced by many methods, namely chemical reactions, physical interactions, or irradiation, depending on the desired properties of the hydrogel. Crosslinking is crucial for controlling the hydrogel's structure, swelling behavior, and responsiveness to external stimuli (Fig. 1).[31] Chemical crosslinking involves the formation of polymer networks through reactions between specific functional groups. The synthesis of hydrogels using this method often leads to superior mechanical strength, tissue adhesion, and stability relative to those formed by physical crosslinking techniques. Common functional groups utilized in chemical crosslinking include amino ($-NH_2$), sulfhydryl ($-SH$), aldehyde ($-CHO$), carboxyl ($-COOH$), and hydroxyl ($-OH$) groups.[32,33] Commonly employed chemical crosslinking strategies encompass processes involving the condensation of aldimine, glutaraldehyde, and carbodiimide. The structures created via this linking approach are often irreversibly formed unless the chemical links are deliberately severed. Chemical crosslinking is particularly beneficial for the development of strong and adhesive hydrogels.[34]

Physical crosslinking occurs through mechanisms such as changes in temperature, pressure, or electric fields, which facilitate the association of polymer chains and lead to the formation of a three-dimensional network structure.[35,36] This approach is advantageous as it typically eliminates the need for chemical crosslinkers, thereby simplifying the process and enhancing environmental sustainability. Nevertheless, the majority of hydrogels created via physical crosslinking exhibit mechanical instability and reversibility. Certain polymer hydrogels demonstrate a sol–gel transition induced by temperature variations, hindering the tangling of polymers. These are designated as hydrogels with thermosensitivity.[37] For example, tissues like the cornea, conjunctiva, and eyelids, which are exposed to external environments, typically manage temperatures from 32 to 34 °C. Sensitive polymers such as poloxamer, poly(N-isopropylacrylamide) (pNIPAM), chitosan (CS), and Pluronic F127 (PF127) are well-known for their ability to form gels at 37 °C. When maintained at room temperature, they remain in the liquid state but a sol–gel transition occurs when in contact with the eye. This unique property enhances their adhesive characteristics, making them ideal for use in ocular treatments.[38]

Physicochemical double crosslinking improves the multifunctional properties of hydrogels. Injectable self-healing hydrogels, developed by using various physical and chemical methods, gained considerable attention and significance in the field of trauma dressing. These hydrogels demonstrate exceptional mechanical strength, self-repair capabilities, adhesion, and biological performance.[39,40] Inspired by the strong adhesive properties of mussels, many multifunctional hydrogels have been developed. Catechol and o-triphenol hydroxyl groups play a crucial role in these designs, providing excellent adhesive properties. The self-healing capability of these hydrogels primarily arises from dynamic physical and chemical interactions. Coordination bonds formed between phenolic hydroxyl groups from catechol or o-phenylene triol compounds and Fe^{3+} ions facilitate dynamic, non-covalent crosslinking. Additionally, reversible Schiff base bonds, a type of dynamic covalent bond, are frequently employed to enhance self-healing characteristics.[41–43] Hydrogels that combine Schiff base bonding with phenolic–Fe^{3+} coordination exhibit faster gelation, improved tissue adhesion, self-rejuvenating properties and strong mechanical features. These features make
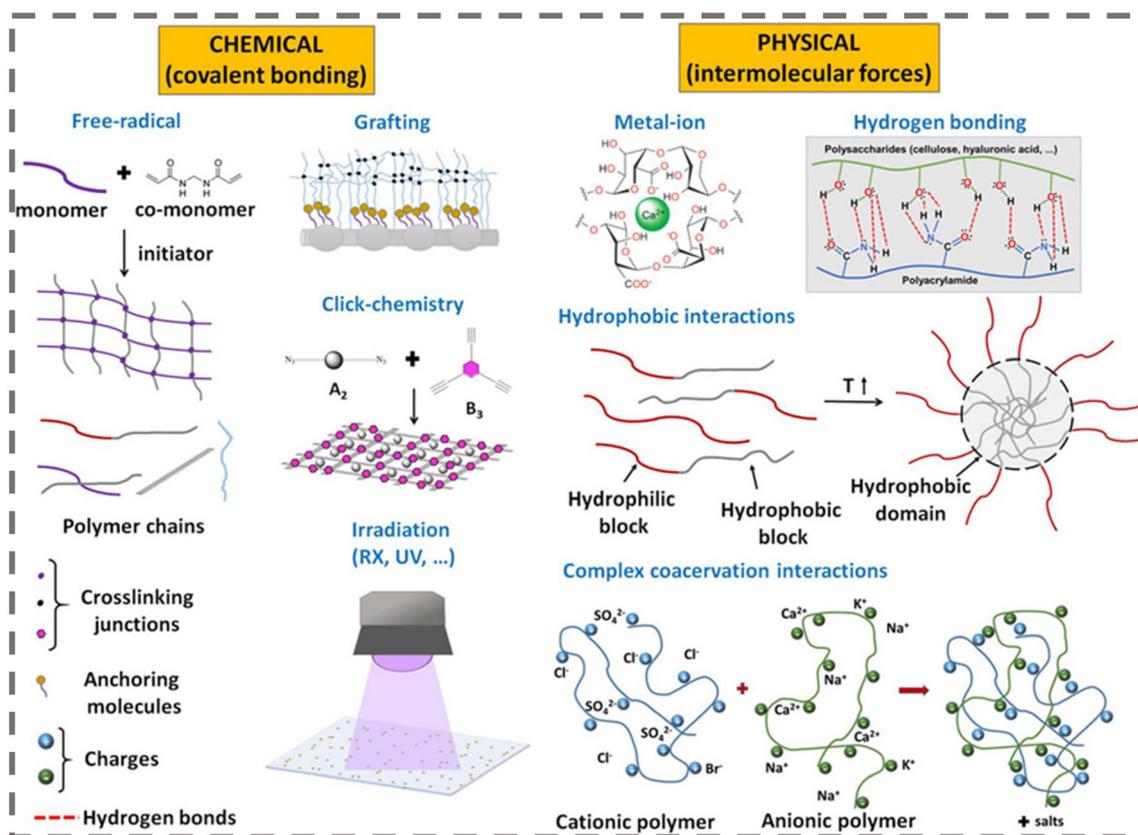
Fig. 1 Schematic illustration of chemical and physical examples of hydrogel cross-linking methods. Reproduced with permission from ref. 31. Copyright 2023 Wiley.

them well-suited for use in challenging and dynamic environments.[44]

2.2 Key functional properties of hydrogels

The performance and clinical utility of hydrogels in advanced wound care and theranostic applications depend on several critical physicochemical and biological properties. For hydrogels to function effectively as intelligent platforms capable of delivering therapeutics, sensing biomarkers, and supporting tissue regeneration, they must demonstrate optimal sensitivity, specificity, biocompatibility, cytotoxicity, and degradability. These properties not only influence therapeutic efficacy but also determine the hydrogel's responsiveness, safety, and adaptability to complex wound environments. (i) Sensitivity is the hydrogel's ability to detect subtle changes in the wound microenvironment, such as pH, glucose levels, temperature, or reactive oxygen species (ROS). In theranostic applications, highly sensitive hydrogels enable real-time biosensing and responsive drug release. For example, glucose-sensitive hydrogels can modulate insulin or drug delivery in diabetic wounds, while pH-responsive systems can release antibiotics selectively in infected sites. Enhanced sensitivity reduces the need for external monitoring devices and supports timely, self-regulating interventions.[45,46] (ii) Specificity refers to the hydrogel's capacity to respond selectively to specific biological stimuli or targets. This property is essential for ensuring accurate detection in biosensing applications and enabling localized drug release at the intended site. In wound healing, specificity enables hydrogels to distinguish between healthy and pathological tissue, supporting targeted therapeutic intervention. For example, hydrogels functionalized with ligands or antibodies can selectively recognize biomarkers of inflammation or infection, thereby facilitating site-specific drug delivery and improving the precision of diagnostic outcomes.[47,48] (iii) Biocompatibility is essential for ensuring that the hydrogel does not provoke adverse immune responses or interfere with the natural healing process. In chronic wounds, biocompatible hydrogels support cellular attachment, proliferation, and migration, which are key processes in tissue regeneration. Natural polymers such as alginate, gelatin, and hyaluronic acid are often used for their inherent biocompatibility, while synthetic polymers are engineered to mimic biological cues and avoid immunogenicity.[49,50] (iv) Minimizing cytotoxicity is essential in the design of multifunctional hydrogels, particularly those incorporating bioactive agents such as drugs, nanoparticles, or photothermal components. These materials must not release toxic byproducts or leachables that could damage surrounding skin cells, such as keratinocytes and fibroblasts, or impede the natural wound healing process. This is especially

critical in the context of chronic wounds, where hydrogels may be applied repeatedly over extended periods. To ensure cellular safety, hydrogel formulations are routinely evaluated using standard *in vitro* assays such as MTT and live/dead staining. These assays help assess cell viability and guide the optimization of material composition, ensuring that the hydrogels are not only effective but also biologically safe for prolonged clinical use.[43,51] (v) Degradability enables hydrogels to break down naturally within the body over time, aligning with the wound healing timeline. Ideally, a hydrogel should degrade into non-toxic, biocompatible byproducts after fulfilling its therapeutic or diagnostic function. Smart degradable hydrogels can respond to wound-specific triggers, such as enzymatic activity or ROS, allowing for controlled, on-demand drug release and minimizing the need for removal. This not only supports tissue remodeling but also enhances patient comfort and compliance.[52,53] The effectiveness of theranostic hydrogels in wound care depends on a delicate balance of sensitivity, specificity, biocompatibility, low cytotoxicity, and controlled degradability. These properties collectively determine the hydrogel's ability to sense, respond, and heal. Optimizing these characteristics ensures precise diagnostics, safe therapeutic delivery, and improved patient outcomes. Continued innovation in smart material design will be pivotal for next-generation wound care solutions.

2.3 Construction strategies for theranostic hydrogels

Developing theranostic hydrogels requires a synergistic approach that combines materials science, biomedical engineering, and responsive design principles. These hydrogels are engineered to fulfill dual diagnostic and therapeutic roles by integrating sensing elements, drug delivery systems, and wound-adaptive biomaterials into a single platform. The construction strategies generally involve three core components: material selection, functionalization techniques, and crosslinking or structural integration methods.[54] (i) Material selection: materials for theranostic hydrogel fabrication must combine biocompatibility and mechanical adaptability. Natural polymers such as alginate, hyaluronic acid, gelatin, and chitosan are ideal due to their inherent biological compatibility and ability to support cell growth and wound healing. Meanwhile, synthetic polymers like PEG, PVA, and Pluronic offer tunable properties such as controlled swelling, degradation, and mechanical strength.[55–58] Inorganic nanoparticles (*e.g.*, gold, silver, or CuS) and carbon-based materials (*e.g.*, graphene oxide) are often incorporated for their photothermal, antimicrobial, or imaging capabilities. Conductive polymers and magnetic nanoparticles further add sensing and tracking capabilities, supporting electrically responsive or magnetically guided diagnostic platforms.[59–61] (ii) Functionalization and targeting: to achieve specificity and responsiveness, hydrogels are functionalized with stimuli-sensitive moieties that react to pH, glucose, ROS, enzymes, or temperature variations mimicking the wound microenvironment.[62] Furthermore, ligands, antibodies, or aptamers can be grafted onto the hydrogel matrix to enable target-

specific recognition, improving both diagnostic accuracy and localized therapy. Fluorescent dyes, MRI contrast agents, and electrochemical sensors are also incorporated for the real-time monitoring of wound status.[63–66] (iii) Crosslinking and integration techniques: crosslinking is pivotal in defining the hydrogel's mechanical strength, degradation profile, and functional stability. Physical crosslinking offers reversible, self-healing features, while chemical crosslinking ensures long-term structural integrity. Emerging methods such as 3D bioprinting, microfluidic patterning, and layer-by-layer assembly are being explored to spatially organize multiple components within a single hydrogel matrix, allowing precise control over drug release kinetics, sensor distribution, and therapeutic compartmentalization.[67,68] The design of theranostic hydrogels involves a multidisciplinary strategy focused on material compatibility, functional integration, and responsive architecture. A clear understanding of these construction principles is essential for developing hydrogels that can simultaneously diagnose, monitor, and treat complex wounds with high precision.

2.4. Wound microenvironment

The largest organ in our body is the skin, which functions as a vital shield protecting internal systems from the outer environment. It plays essential roles in discerning external stimuli, regulating body temperature, and shielding from potential stress. Given its constant exposure to external factors, the skin is particularly susceptible to damage.[69,70] While minor skin injuries often heal over time, restoring the skin's original appearance, complete functional recovery, similar to that of infant skin, is challenging in adults.[71] Skin repair and healing is a highly impeding mechanism with four main stages: proliferation, inflammation, remodeling and homeostasis. These phases work together to restore tissue integrity, with each stage playing a crucial part in the repair and regeneration of tissues. Coordination of cellular events across these phases ensures optimal recovery of the skin. Hemostasis is initiated immediately after an injury, with red blood cells, fibrin, and platelets working together, giving rise to the clotting of blood. In the phase of subsequent inflammation, chemokines released by platelets attract immune cells such as monocytes, lymphocytes, neutrophils, macrophages *etc.* to the major wound site. These cells liberate a variety of enzymes, cytokines and growth factors to support the complete healing process. In the proliferation phase, epidermal cells, fibroblasts and endothelial cells migrate towards the wounded region, multiply, and differentiate, facilitating the repair of granulation tissue and regeneration of blood vessels, and re-epithelialization. The final phase, also known as the remodeling phase focuses on restoring the structural and functional nature of the wound region. This involves the formation of myofibroblasts from fibroblasts, lessening of excess blood vessels, clearing inflammation, and the reconstruction of the extracellular matrix (ECM). Any disruption to these phases may result in abnormal healing of chronic wounds with prolonged development of hypertrophic scars and keloids due to excess proliferation and

inflammation. However, this process is rarely flawless, as disruptions at any stage—caused by factors such as excessive inflammation, severe burns, extensive tissue loss, infections, or conditions like diabetes—can hinder appropriate wound repair and recovery (Fig. 2a–d).[72–75]

3. Hydrogels in modern wound management: insights from recent studies

3.1 Hydrogels for bacterial wounds

Effective wound care is crucial for preventing infections and accelerating tissue repair. Infections by pathogenic bacteria significantly impair healing and can pose severe health risks, especially in chronic or immunocompromised patients. The rise of antibiotic resistance and the limited effectiveness of conventional dressings have prompted the development of advanced hydrogel-based materials. Hydrogels, due to their high-water content, tunable physicochemical properties, and ability to encapsulate functional agents, are emerging as prom-

ising alternatives. Their antibacterial action typically depends on direct contact with microbes, but they also serve as delivery platforms for photothermal agents, antibiotics, and ROS-generating systems. To elucidate advances in this domain, we categorize hydrogel innovations based on their core therapeutic modality: PTT, photodynamic therapy (PDT), chemotherapy-based release, and multimodal combination therapies.[76,77] Wang *et al.* introduced a hydrogel utilizing MXene, a two-dimensional carbonitride material, as a substrate. They reduced silver nanoparticles (AgNPs) *in situ* and polymerized polydopamine (PDA) on MXene's surface to create a photothermal agent (PTA), MXene-Ag-PDA. This agent was incorporated into a hydrogel matrix composed of the cationic polymer acrylamide-1-(4-vinylbenzyl)-3-methylimidazolium bromide-acrylamidophenylboronic acid (AM-VBIMBr-AAPBA), quaternary ammonium chitosan (HACC), and oxidized sodium alginate (OSA). Following crosslinking, they developed the poly(*N*-vinyl-lacetamide-*co*-octadecyl methacrylate)/MXene-Ag-PDA (PNVAO/ M-A-P) multifunctional hydrogel, which demonstrated both PTT properties and intrinsic antibacterial effects. The cationic groups within the hydrogel interacted electrostatically with bacteria, helping to eliminate them. Furthermore, exposure to
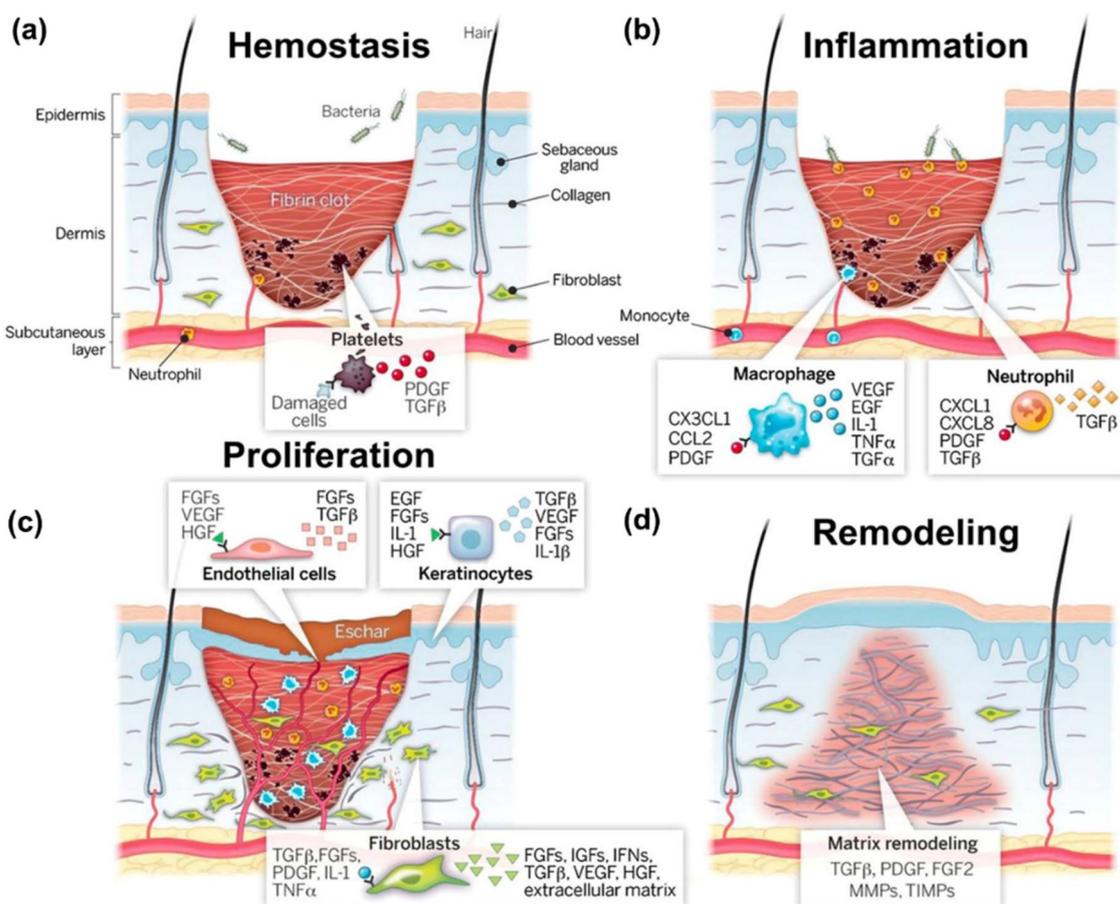

Fig. 2 Schematic illustration of the four stages of wound healing: (a) hemostasis, (b) inflammation, (c) proliferation, and (d) remodeling. Reproduced with permission from ref. 72. Copyright 2021 American Chemical Society.

NIR light (808 nm, 0.5 W cm^{-2}) generated localized heat, further enhancing bacterial destruction, reducing bacterial survival, speeding up the antibacterial process, and healing the dynamic wound environment (Fig. 3a).[78] A similar study designed OSA-grafted dopamine (DA), carboxymethyl CS, and Fe^{3+} ions (OSD/CMC/Fe), with the addition of PDA-loaded poly(thiophene-3-acetic acid) (PA) to form OSD/CMC/Fe/PA hydrogels. Their structure relies on dynamic Schiff base and Fe^{3+} coordination bonds, which enable self-healing and allow the hydrogel to adapt to irregular wound surfaces. The OSD/CMC/Fe/PA hydrogel exhibits strong antibacterial properties, conductivity, and PTT effects under NIR light (808 nm, 1.4 W cm^{-2}) making it versatile for wound applications (Fig. 3b and c).[79] He *et al.* developed innovative nanocomposite hydrogels that were conductive, self-healing, and adhesive, showcasing strong PTT antibacterial properties. These hydrogels, made from benzaldehyde-terminated PF127/carbon nanotubes (PF127/CNTs) and *N*-carboxyethyl CS (CEC), effectively promoted PTT under an 808 nm laser (1.4 W cm^{-2}) for treating infected wounds. They exhibited rapid gelation, durable mechanical strength, hemostatic capabilities, and high-water absorption while being biodegradable. Additionally, when loaded with moxifloxacin hydrochloride, the hydrogels demonstrated pH-responsive drug release and robust antibacterial activity. Their adhesive nature enabled effective hemostasis in mouse models of liver trauma and tail amputations. Incorporating CNTs enhanced their PTT antimicrobial efficacy and conductivity (Fig. 3d).[80] Zhang *et al.* developed effective dressings for infected burn wounds at joints; a hydrogel dressing (PBEC) was created using PVA, epigallocatechin gallate, anhydrous sodium borax, and copper chloride. The PBEC hydrogel demonstrates excellent adhesion to various surfaces, impressive stretchability, and rapid self-repair when damaged. Moreover, it exhibits properties such as scavenging ROS, photothermal sterilization, hemostatic activity, and biocompatibility. The hydrogel notably enhances wound healing, particularly when combined with 808 nm NIR irradiation (Fig. 3e).[81] Supramolecular hydrogels with antibacterial, antioxidant, self-healing, and tissue-adhesive properties are highly desirable for treating bacteria-infected wounds. The supramolecular hydrogels are based on ureidopyrimidinone, poly(glycerol sebacate)-*co*-poly(ethylene glycol)-*g*-catechol (PEGSDU), and mesoporous copper sulfide NPs using quadruple hydrogen bonds and catechol–Cu coordination. Under an 808 nm laser, supramolecular hydrogels exhibit excellent antibacterial, antioxidant, and tissue-adhesive properties, making them effective at managing methicillin-resistant *Staphylococcus aureus* (MRSA)-infected wounds (Fig. 3f).[82] Furthermore, a multifunctional composite hydrogel has been reported, exhibiting strong adhesion, self-healing capability, and dual antimicrobial properties, thereby contributing to improved wound healing outcomes. This hydrogel was synthesized using PVA, CA, and PDA NPs, confirming its excellent bioactivity and PTT (808 nm, 0.6 W cm^{-2}) effectiveness in promoting rapid wound repair.[83] Wang *et al.* developed a multifunctional treatment platform by incorporating nanodiamonds (NDs), known for their excellent biocom-

patibility, into a solution of acrylic-grafted CS (CEC) and oxidized hyaluronic acid (OHA), resulting in the CEC-OHA-ND hydrogels. These hydrogels demonstrate rapid hemostatic properties, PTT effects under an 808 nm laser promote wound healing, and they possess remarkable self-healing and injectable capabilities.[84] Another study developed a drug-free hydrogel designed to accelerate the healing of bacteria-infected wounds. The hydrogel was formulated using modified polysaccharides and humic acid (HU), with HA oxidized to introduce aldehyde groups and pectin (PT) functionalized with amino groups *via* an amidation reaction. HU was further reduced to enhance its phenolic hydroxyl and catechol contents, boosting its antioxidant, hemostatic, antibacterial, and PTT properties. The final HA-PT/HUOH hydrogel was assembled through hydrogen bonding and dynamic Schiff base cross-linking, making it a promising wound healing material. The HA-PT/HUOH hydrogel demonstrated exceptional PTT (808 nm, 2 W cm^{-2}) properties, rapid self-healing, robust bioadhesion, and outstanding injectability. This multifunctional hydrogel provides a promising, drug-free solution for wound dressings in clinical applications.[85] Other work explored the incorporation of porphyrinic metal–organic framework (MOF) crystals into GelMA to create a photocurable composite resin. The goal was to enable the fabrication of customized wound dressings using vat photopolymerization 3D printing. By integrating MOF crystals, the composite resin gained enhanced functionality, making it suitable for advanced wound care. Furthermore, the printed materials are endowed with PTT and PDT functionalities as a result of the MOF crystals. Antibacterial tests demonstrated the potent bactericidal effects of the GelMA/MOF hydrogels under PTT and PDT activation. After 30 min of light exposure ($\sim$30 mW cm^{-2}, $\lambda \geq 420$ nm), the hydrogel with the highest MOF concentration exhibited an antibacterial efficacy of over 99.99% against both *Staphylococcus aureus* (*S. aureus*) and *Escherichia coli* (*E. coli*). This research presented a novel approach for combining photosensitive MOFs with 3D printing to develop customizable PTT/PDT monoliths and patches, offering new possibilities for personalized wound care treatments.[86] Ma *et al.* pioneered the development of an antibacterial dressing that was capable of effectively eliminating bacteria by employing an aggregation-induced emission (AIE)-active photosensitizer, DTTPB. The D–π–A structure of DTTPB facilitates the efficient synthesis of ROS in its aggregated form, thereby surpassing the constraints of conventional photosensitizers. DTTPB is integrated with Carbomer 940 to make an injectable hydrogel dressing (DTTPB@gel). This hydrogel adheres well to wound sites and retains the antimicrobial efficacy of DTTPB, enhancing its wound-healing capabilities under white light at 36 mW cm^{-2}.[87]

Gallium ions possess a unique mechanism that disrupts bacterial iron metabolism, making them highly effective at treating bacterial infections. This study successfully developed hydrogels by crosslinking konjac glucomannan and polyacrylamide (KGM/PAM) with gallium ions (Ga^{3+}), resulting in hydrogels with excellent swelling capacity, suitable mechanical strength, and controllable degradation properties. Ga^{3+}, acting
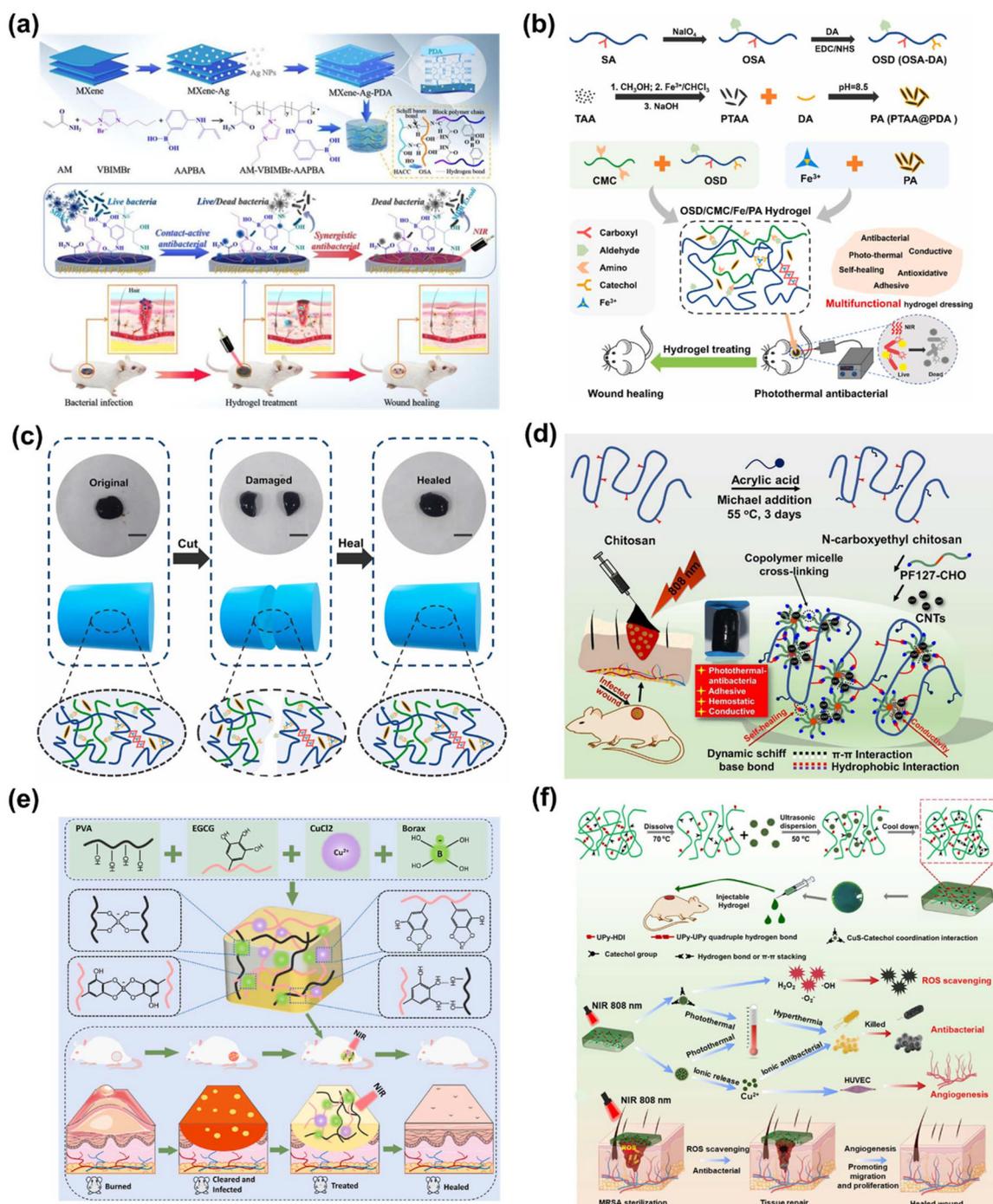
Fig. 3 (a) Schematic illustration of the composite hydrogel synthesis process, highlighting the integration of bioactive components and hydrogel application on an infected skin wound in a mouse model, demonstrating the hydrogel's role in promoting healing through antimicrobial and regenerative functions. Reproduced with permission from ref. 78. Copyright 2025 Elsevier. (b and c) Illustration of a self-healing hydrogel wound dressing that is antibacterial and conductive, and is characterized by dual dynamic bonds. Reproduced with permission from ref. 79. Copyright 2023 Elsevier. (d) Schematic representation illustrating the preparation of the CEC/PF/CNT hydrogel, highlighting its strong adhesion properties, and enhancing its functionality for application on an infected wound. Reproduced with permission from ref. 80. Copyright 2020 Wiley. (e) A schematic illustration outlining the design strategy for the PBEC multifunctional hydrogel, aimed at promoting healing in infected deep second-degree skin burn wounds, particularly in joint areas and wound care in sensitive regions. Reproduced with permission from ref. 81. Copyright 2024 American Chemical Society. (f) Schematic representation of the preparation and application of PEGSDU/CuS. Reproduced with permission from ref. 82. Copyright 2024 Elsevier.

as a crosslinking agent, enhances the hydrogels' stability and significantly boosts their antibacterial properties, creating innovative KGM/PAM/Ga^{3+} hydrogels for wound treatment. Evaluations of antibacterial efficacy and biocompatibility reveal that these hydrogels effectively suppress bacterial growth through the sustained release of Ga ions, while exhibiting minimal cytotoxicity and excellent blood compatibility. The wound healing performance of KGM/PAM/Ga^{3+} hydrogels markedly accelerates the tissue regeneration and healing of infected wounds.[88] A nanocomposite hydrogel system reinforced with halloysite clay intercalated with quercetin (Q), hyaluronan, and Ag NPs (HAQ-Hal-Ag) has been reported for wound dressing applications. HAQ-Hal-Ag was incorporated into a fungal carboxymethyl CS (FC) and polyacrylamide (PAM) matrix (FC-PAM) using methylene bisacrylamide (MBA) cross-linker and ammonium persulfate (APS) as the initiator. The hydrogels exhibited enhanced compressive strength, reaching 1.04 MPa at 5 wt%, along with a porous structure, excellent swelling capacity, and notable antibacterial activity against both *E. coli* and *S. aureus*.[89] GelMA-NBNAGA was formed by grafting photosensitive monomers of *N'*-(2-nitrobenzyl)-*N*-acryloyl glycinamide (NBNAGA) onto methacrylated gelatin (GelMA) through Michael addition. A single phase of ultraviolet (UV) light irradiation was used to produce the hydrogel within seconds. The dual-reinforced hydrogels exhibited enhanced mechanical properties compared to those with only chemical or physical cross-linking. Hydrophobic drugs, specifically the anticancer agent doxorubicin (DOX) and the antibiotic rifampicin (Rif), were successfully loaded into the hydrogels. *In vitro*, antimicrobial tests demonstrated the hydrogel's effectiveness against *E. coli* and *S. aureus* bacteria. NBNAGA-modified GelMA hydrogel shows promise as a wound dressing material capable of on-demand delivery of hydrophobic antibiotics.[90] Poly(thioctic acid) (PTA), PDA, and curcumin (Cur) were combined to create multifunctional hydrogels by Feng *et al.* The hydrogels exhibited exceptional bioadhesive and self-healing properties as a result of the covalent and hydrogen bonds that were established between PTA, PDA, and Cur. These hydrogels were employed as bandages for wounds infected with *S. aureus*. Among them, the PDA-PTA-Cur 16 hydrogel exhibited superior performance in terms of stability, antioxidant activity, and antibacterial efficacy. This hydrogel improved the healing of infected lesions by suppressing bacterial growth, reducing inflammation, promoting collagen formation, and facilitating angiogenesis, as evidenced by *in vivo* experiments.[91] Multifunctional injectable hydrogels derived from polysaccharide matrices have demonstrated multifunctionality, particularly their capacity to neutralize bacteria through integrated antibacterial mechanisms. Furthermore, the polymer matrix was developed using dynamic and reversible coordination bonds between Ag^{+} ions and functional groups such as carboxyl, amino, or hydroxyl on CMC. Additionally, hydrogen bonding and electrostatic interactions contributed to its structural integrity. This design facilitated the integration of sodium nitroprusside (SNP)-loaded PCN-224 NPs. The SNP@PCN@Gel hydrogels that were produced exhibited a porous structure that was interconnected, exceptional self-healing capabilities, and strong antibacterial properties. SNP@PCN@Gel is capable of generating ROS, nitric oxide (NO), and Fe^{2+}, along with a sustained release of Ag^{+}, which collectively contribute to effective bacterial eradication *via* synergistic PTT (660 nm, 0.4 W cm^{-2}). This approach presents a novel method for creating photoactivatable "all-in-one" hydrogels with enhanced antibacterial effects, offering a promising alternative to traditional antibiotics and advancing wound dressing development (Fig. 4a).[92] These modality-driven classifications provide a clearer understanding of how hydrogel systems are tailored for specific therapeutic functions. Such strategic design advances offer promising solutions for managing complex and drug-resistant bacterial wound infections.

Zhou. *et al.* developed a peptide hydrogel derived from the natural antimicrobial peptide Jelleine-1 for treating MRSA-infected wounds. It exhibited broad-spectrum antimicrobial properties, biodegradability, and excellent biocompatibility. In a mouse model of MRSA-infected burn wounds, the hydrogel significantly promoted wound healing. This innovative antimicrobial dressing provides a promising, antibiotic-free approach for treating drug-resistant bacterial infections and highlights the potential of antimicrobial peptides in wound care.[93] A recent study developed an antibacterial hydrogel, PNVBA, with antifreeze and anti-drying properties using 1-butyl-3-vinylimidazolium bromide (VBIMBr), *N*-isopropylacrylamide (NIPAM), and 3-acrylamidophenylboronic acid (AAPBA). The PNVBA hydrogel demonstrated a high bovine serum albumin (BSA) adsorption capacity of 280 mg g^{-1}, a 98% sterilization rate against *E. coli* and MRSA, and excellent biocompatibility with a 90% cell survival rate in L929 cells. These features highlight its potential as an effective, durable wound dressing.[94] MRSA is a major cause of wound infections, posing significant treatment challenges. Infected wounds often develop acidic environments with a pH range of 4.5 to 6.5. Endolysin LysSYL, derived from phage SYL, has shown potential as an antistaphylococcal agent. However, endolysins typically suffer from instability and low bioavailability under acidic conditions. This report introduced a series of self-assembling peptides, with peptide L5 selected for its gel-forming ability and enhanced bioavailability. L5 demonstrated a pH-responsive antimicrobial effect at pH 5.5 and formed biocompatible hydrogels at neutral pH (7.4). When loaded with LysSYL, the L5@LysSYL hydrogel showed improved thermal stability and a controlled release of LysSYL. This hydrogel effectively eradicated *S. aureus* by disrupting bacterial membranes and inhibiting cell separation. In a mouse model of MRSA-infected wounds, L5@LysSYL hydrogels significantly promoted wound healing (Fig. 4b).[95] Wound infection significantly hinders the healing process, impacting both the speed and quality of recovery. Although hydrogen peroxide (H$_2$O$_2$) is known for its antibacterial properties and ability to promote wound healing, its application requires precise dosing to avoid delays in healing. Huang *et al.* developed a calcium peroxide-
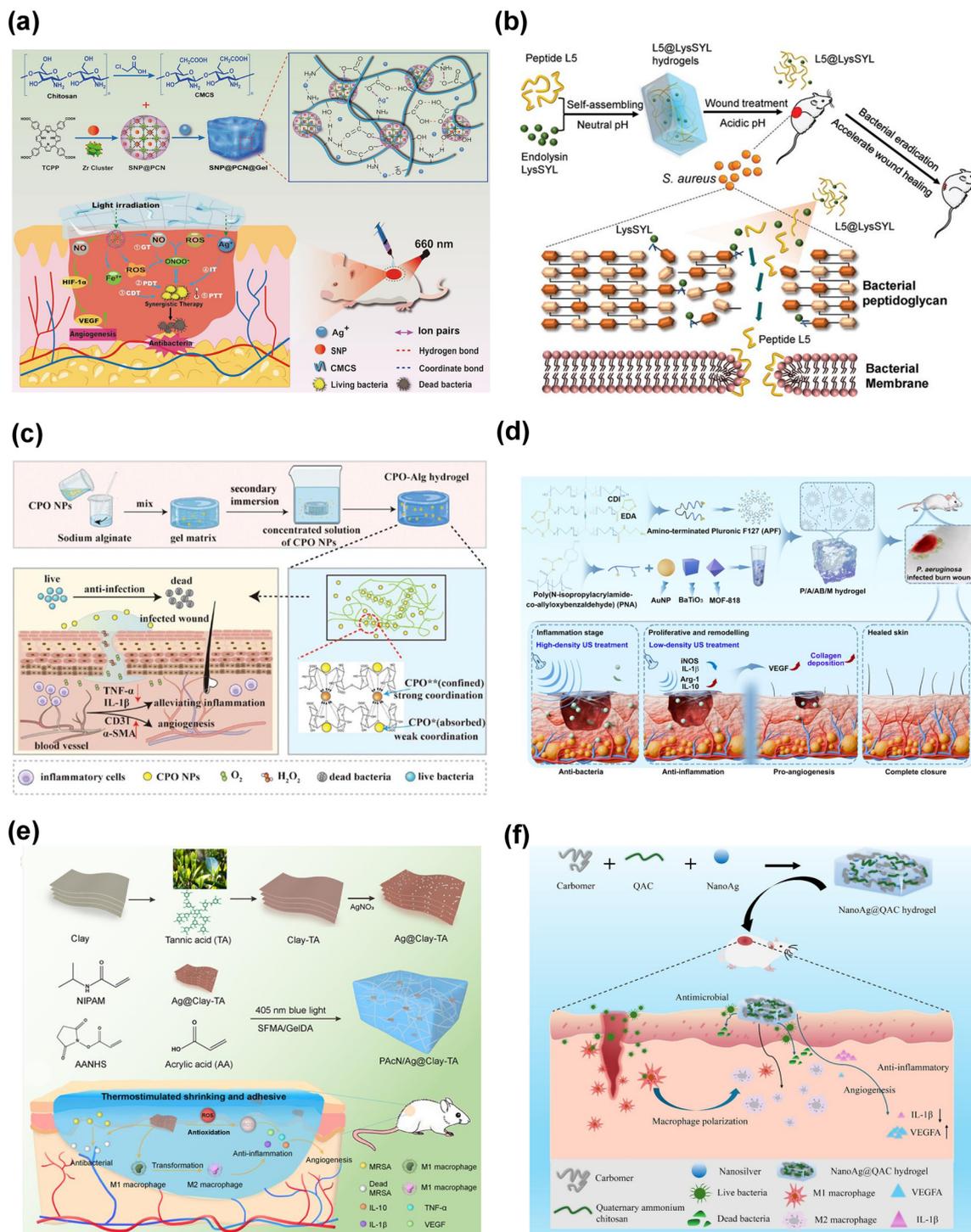
Fig. 4 (a) The fabrication procedure for SNP@PCN@Gel hydrogels and a depiction of the mechanisms behind synergistic therapies, including PTT, PDT, CDT, GT, and ion therapy. Reproduced with permission from ref. 92. Copyright 2024 Springer Nature. (b) Schematic diagram illustrating the development of pH-sensitive, self-assembling endolysin LysSYL-loaded peptide L5@LysSYL hydrogels designed for infected wounds. Reproduced with permission from ref. 95. Copyright 2024 Wiley. (c) Schematic diagram demonstrating the preparation of CPO-Alg hydrogel and its application in enhancing the wound healing process. Reproduced with permission from ref. 96. Copyright 2024 Wiley. (d) An illustration showing the preparation of P/A/AB/M hydrogel, which is applied to promote the repair of *P. aeruginosa*-infected full-thickness burn wounds. Reproduced with permission from ref. 97. Copyright 2025 Elsevier. (e) Schematic illustration presenting the fabrication of PAcN/Ag@Clay-TA hydrogel. This hydrogel dressing is designed for diabetic wound healing and effectively combats MRSA infections, promoting accelerated recovery. Reproduced with permission from ref. 99. Copyright 2024 Elsevier. (f) Schematic diagram depicting the NanoAg@QAC hydrogel formulated for the treatment of infected diabetic wounds. Reproduced with permission from ref. 100. Copyright 2025 Elsevier.

based hydrogel (CPO-Alg hydrogel) designed to deliver a controlled, biphasic release of H_2O_2, providing potent initial antibacterial activity, followed by sustained support for cell proliferation and wound healing. The hydrogel is designed to incorporate calcium peroxide (CPO) NPs in two distinct regions within the gel structure. Upon application to infected wounds, CPO NPs with weak binding are quickly released, targeting bacterial and biofilm areas at high concentrations to effectively eliminate pathogens. Meanwhile, the more tightly bound CPO NPs within the gel slowly degrade and release H_2O_2 in a controlled manner through hydrolysis in the moist wound environment, fostering cellular growth during the later stages of healing. The CPO-Alg hydrogel provides a novel and effective approach for managing chronic wounds, offering promising potential for enhancing wound healing outcomes (Fig. 4c).[96] Yu *et al.* proposed a thermosensitive hydrogel crosslinked with pNIPAM-*co*-allyloxybenzaldehyde (PNA) and PF127 *via* a Schiff base reaction. A multifunctional nanocomposite hydrogel dressing was developed by integrating piezoelectric AuNPs with barium titanate ($Au@BaTiO_3$) and the antioxidant MOF-818. This hydrogel showed stable gel properties over a wide temperature range, excellent self-healing, and the ability to generate ROS under ultrasound stimulation, thanks to $Au@BaTiO_3$'s piezoelectric properties. This combination facilitated fibroblast proliferation and migration and enhanced anti-inflammatory macrophage polarization under ultrasound (Fig. 4d).[97] Zhu and colleagues developed innovative composite hydrogels made from *Capparis spinosa* L. extract (CSL) with sodium alginate (SA), utilizing calcium chloride ($CaCl_2$) as a safe ionic crosslinker for biomedical purposes. The composite hydrogels were extensively evaluated for their swelling capacity, antioxidant activity, water retention, biocompatibility, and antibacterial efficacy.[98] Similar work developed an adhesive and temperature-sensitive hydrogel for chronic wounds. This hydrogel is composed of *N*-isopropylacrylamide (NIPAM), polyacrylic acid (PAA), and *N*-hydroxysuccinimide ester, dopamine (DA)-modified gelatin and silver (Ag)-coated clay-TA NPs. This multifunctional dressing exhibited strong tissue adhesion along with antibacterial and antioxidant properties (Fig. 4e).[99] The NanoAg@QAC hydrogel combines NanoAg with quaternary ammonium chitosan (QAC), offering ideal wound dressing properties such as strong mechanical strength, antimicrobial and anti-biofilm activity, and cytocompatibility. *In vivo* studies showed its effectiveness against *S. aureus* and *P. aeruginosa* infections, promoting early-stage wound closure and healing properties (Fig. 4f).[100] Cheng *et al.* developed innovative calcium NPs (CaNPs) and incorporated them into a hydrogel made from gelatin (Gel) with guar gum (GG) to create a new hydrogel, GG@Gel-Ca. This hydrogel was designed to enhance hemostasis, provide antibacterial properties, and promote wound healing. The GG@Gel-Ca hydrogel exhibited excellent swelling behavior, strong antibacterial activity, superior hemocompatibility and hemostatic properties, as well as outstanding cytocompatibility.[101] Jallab *et al.* presented the develop-

ment of a wound dressing hydrogel incorporating non-oxide copper nanowires and a PVA/CS matrix crosslinked with tetraethyl orthosilicate (TEOS), the flexibility of which was further enhanced by adding glycerol. This hydrogel demonstrated excellent mechanical properties due to the presence of the nanowires, a tensile strength of 58.76 MPa, and an elongation of 124.78%. In wound healing tests, the hydrogel promoted significant wound closure, and healing within 72 h in HDF cells. Furthermore, antibacterial tests using the 96-well microdilution method showed strong antibacterial effects, with inhibition ranging from 50 to 97% against *E. coli* and *S. aureus*.[102] A recent study introduced an innovative asymmetric composite dressing inspired by the dual-layer structure of traditional Chinese medicinal plaster patches for chronic wound care. This dressing integrates electrospun poly(lactic acid-*co*-trimethylene carbonate) (PLATMC) nanofibers with a GelMa hydrogel containing epinecidin-1@CS (Epi-1@CS) NPs, creating a temperature-responsive self-contracting nanofiber/hydrogel (TSNH) hydrogel composite. The nanofiber layer provides structural support and promotes wound healing, while the hydrogel layer enhances cytocompatibility and offers anti-inflammatory, antioxidant, and antibacterial benefits. This TSNH dressing holds significant potential for treating chronically infected wounds effectively.[103] Furthermore, other research presented a CS-based hydrogel film, cross-linked with a polycationic peptide conjugated with graphene-Ag (CGrAP) nanocomposite, intended for antibacterial (*S. aureus*) wound management. The CGrAP hydrogel was generated by a Schiff base reaction between ε-poly-L-lysine functionalized graphene-Ag nanocomposites and CS, which was later fabricated as a film. The antibacterial mechanism is based on electrostatic interactions and the formation of ROS, leading to the breakdown of bacterial cells. *In vivo*, experiments utilizing an animal model indicated that the CGrAP hydrogel exhibited enhanced bacterial elimination and wound healing relative to conventional antibiotic therapies.[104] The development of multifunctional hydrogels for bacterial wound treatment marks a significant advancement in wound care, integrating antimicrobial, hemostatic, and regenerative functionalities into single platforms. Particularly, hydrogels leveraging photothermal, photodynamic, and combination therapies have shown remarkable efficacy for infection control and tissue repair. Continued innovation in stimuli-responsiveness, biocompatibility, and targeted drug delivery will be essential for translating these systems into effective clinical treatments for complex and drug-resistant wound infections.

3.2 Hydrogels for diabetic wounds

Hydrogels are well-suited for various biomedical uses, particularly in wound management. Diabetic individuals often experience slow-healing wounds due to compromised cellular function. Hydrogels provide an effective approach for supporting healing by preserving moisture and enabling the delivery of therapeutic substances.[105] Protein-based hydrogels often suffer from weak mechanical properties and limited biological

functionality. Liu *et al.* developed a novel protein–protein hydrogel crosslinked with BSA and collagen-like protein (CLP) through Ag–S bonds. This innovative approach enabled the creation of a stable and functional hydrogel. The resulting hydrogel demonstrated excellent plasticity, self-healing properties, and a redox-responsive gel–sol transition. Compared to BSA-only hydrogels, the protein–protein hydrogel showed improved cellular viability and enhanced cell migration. *In vivo* studies confirmed its effectiveness at promoting wound healing, with accelerated recovery observed in diabetic mouse models and zebrafish with UV-induced burns. Analysis of proinflammatory cytokines and epidermal differentiation proteins further validated its role in wound repair, highlighting its potential for advanced wound care applications.[106] Uncontrolled diabetes can lead to the development of diabetic foot ulcers, which require biocompatible wound healing strategies. This study developed biomatrices using semi-interpenetrating polymer networks (SIPNs) made from polyurethane, collagen, and dextran. SIPNs with 10%, 20%, and 30% dextran concentrations displayed porous structures with high degrees of crosslinking, up to 94%, due to hydrogen bonding. These hydrogels showed improved mechanical strength, swelling capacity, and resistance to degradation. In diabetic rat models, the hydrogels significantly speed up wound healing, with the 20% dextran hydrogel achieving full wound closure within 21 days. These findings underscore the ability of hydrogels to aid in wound healing by minimizing inflammation and encouraging tissue regeneration, while maintaining skin safety. Hydrogels demonstrate promising therapeutic potential for effective wound care.[107] A recent study developed on-demand degradable hydrogels with multiple responsive features. These hydrogels were synthesized using selenol–dichlorotetrazine nucleophilic aromatic substitution (SNAr) reactions in a mild buffer solution, eliminating the need for additional additives or post-synthesis treatments. The reaction between selenol and tetrazine forms three degradable bonds—diselenide, aryl selenide, and dearomatized selenide—in a single step. The resulting hydrogels are highly adaptable to various environments, exhibiting self-healing properties, controlled degradation, and light-induced antibacterial effects (Fig. 5a).[108] Guo *et al.* introduced an innovative hybrid hydrogel dressing, crosslinked with dynamic borate bonds, that featured PTT properties designed to enhance the diabetic wound healing process without the need for additional medications. This hydrogel is composed of phenylboronic acid modified with CS and HA, crosslinked with TA through borate bonds, and includes Prussian blue NPs (PBNPs) for a PTT response under the 808 nm laser (0.5 W cm^{-2}). Its unique design enhances both therapeutic and functional properties for targeted applications. The hydrogel demonstrates broad-spectrum antioxidant activity due to the synergistic effects of borate bonds, TA, and PBNPs. Additionally, HA contributes to the modulation of macrophage phenotypes, aiding in the transformation of the inflammatory environment typical of diabetic wounds. The PTT effect of PBNPs further promotes angiogenesis, leading to enhanced epithelialization and collagen

deposition. This multifunctional hydrogel system effectively supports all phases of wound healing by mitigating oxidative stress, modulating immune responses, and promoting angiogenesis, showcasing significant potential for diabetic wound care applications (Fig. 5b).[109] Diabetic foot ulcers present a major healthcare challenge due to excess ROS production and unresolved inflammation. This is largely caused by macrophages failing to transition from the pro-inflammatory M1 to the healing M2 phenotype. To address this, an injectable dextran methacrylate DMM/GelMA hydrogel has been developed to modulate macrophage metabolism by inhibiting succinate dehydrogenase (SDH) activity and promoting macrophage repolarization. *In vitro*, the hydrogel reduced ROS levels, inflammation, and succinate dehydrogenase (SDH) activity in macrophages. *In vivo*, it enhanced wound healing in diabetic mice by promoting collagen deposition and tissue regeneration, while simultaneously reducing inflammation and inducing macrophage polarization toward the pro-healing M2 phenotype. This hydrogel demonstrates considerable promise in the treatment of diabetic wounds, offering effective healing properties. Its unique formulation supports tissue repair and enhances wound recovery.[110] Li *et al.* developed a layered hydrogel dressing incorporating a continuous biochemical gradient of glycyrrhizic acid designed to regulate immunomodulatory responses in diabetic wound healing (Fig. 5c).[111] Collagen extracted from eggshell waste holds promise for wound healing, but often lacks mechanical strength. To overcome this, collagen was incorporated into an alginate-based hydrogel (AC-hydrogel). Calcium carbonate (CaCO$_3$) and collagen were extracted *via* calcination and ultrasonication. Furthermore, *in vitro* and *in vivo* models demonstrated that AC-hydrogel significantly improved wound healing in diabetic models, highlighting its potential for clinical applications.[112] Exosomes are emerging as a promising tool in wound healing research, as they promote blood circulation and endocrine signaling. Their ability to enhance cell regeneration makes them valuable for advanced therapeutic applications. Recent studies have shown that hydrogels, when combined with exosomes, can significantly accelerate wound healing through noninvasive application. Britton *et al.* developed a series of single-domain protein-based hydrogels that exhibited physical crosslinking and upper critical solution temperature (UCST) properties. Among these, the hydrogel variant Q5, optimized for superior UCST characteristics and faster gelation rates, was chosen for the encapsulation and release of exosomes, termed Q5Exo. This formulation demonstrated rapid gelation and notably reduced wound healing time, indicating its foundation for future hybrid, noninvasive protein-exosome therapies.[113] Maintaining effective glycemic control is crucial for promoting optimal wound healing in diabetic patients. Conventional antibacterial and anti-inflammatory treatments, while essential, often fail to adequately address the hyperglycemic conditions characteristic of diabetic wounds. Consequently, the search for innovative therapeutic approaches for accelerating diabetic wound healing has gained significant momentum. Covalent organic frameworks (COFs), a novel class of crystalline porous
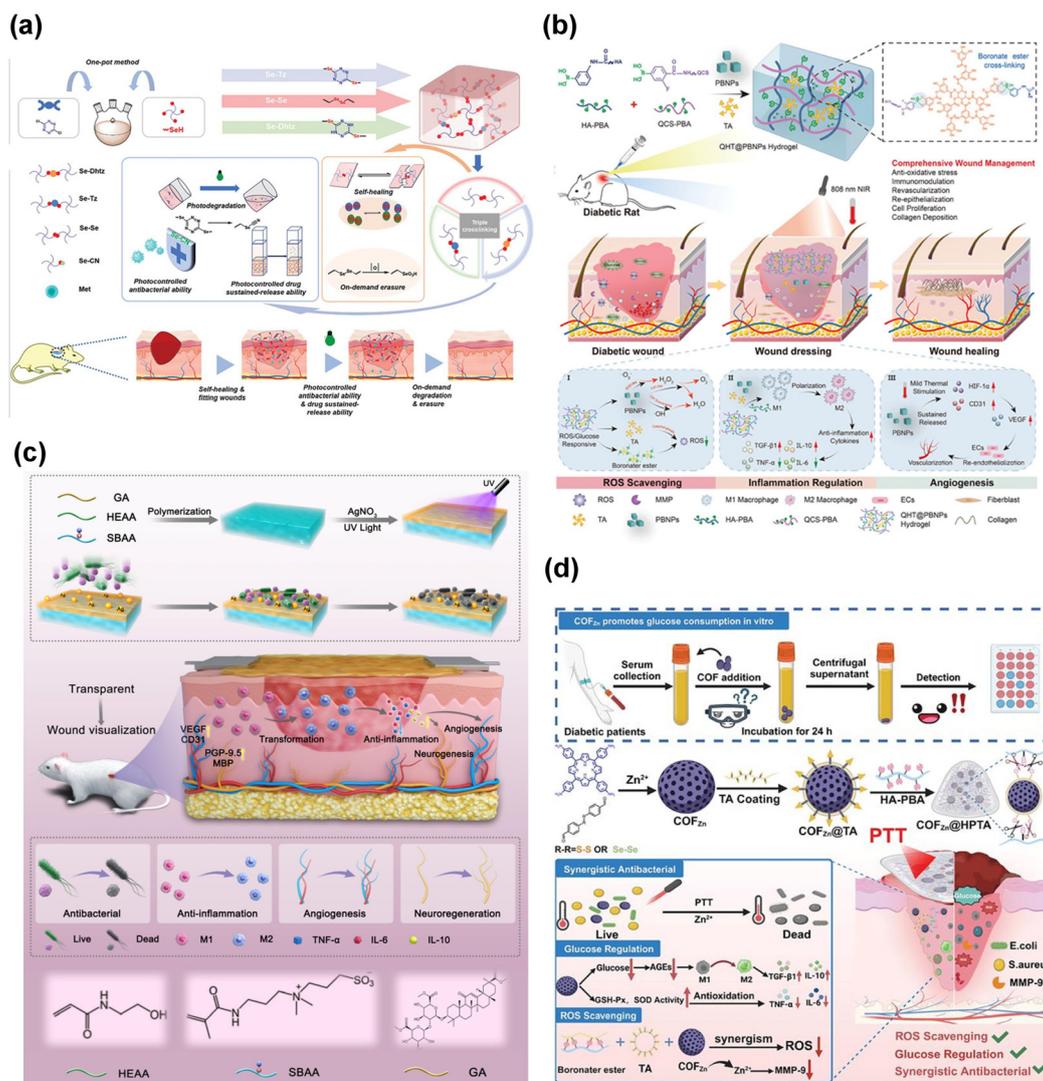
Fig. 5 (a) The Se-Tz hydrogel is created using a one-step method that combines selenol and tetrazine. It incorporates three types of chemical cross-links (diselenide, aryl selenide, and dearomatized selenide bonds), granting it unique features of photocontrolled release and self-healing. Animal studies also demonstrated its light-activated antibacterial effects. Reproduced with permission from ref. 108. Copyright 2024 Wiley. (b) Schematic representation of the synthesis of QHT@PBNP hydrogel and its therapeutic mechanisms, including ROS scavenging, inflammation modulation, and angiogenesis promotion, facilitating diabetic wound healing. Reproduced with permission from ref. 109. Copyright 2025 Wiley. (c) Schematic illustration demonstrating the fabrication process and application of the multifunctional HGAS hydrogel. Reproduced with permission from ref. 111. Copyright 2024 Elsevier. (d) Schematic diagram depicting the synthesis of the COFZn@HPTA hydrogel and its mechanism for the simultaneous diagnosis and treatment of diabetic wounds through co-incubation. Reproduced with permission from ref. 114. Copyright 2025 Wiley.

polymers formed through robust covalent bonds, offer exceptional structural tunability, making them an ideal platform for advanced therapeutic applications. This study presented the development of two redox-responsive Zn(II)-coordinated porphyrin COF hydrogels, which have shown the capability to rapidly reduce blood glucose levels in localized tissues. These hydrogels also enhance angiogenesis, scavenge ROS, and exhibit PTT antimicrobial properties, effectively managing infections and promoting wound healing in the hyperglycemic environment typical of diabetic patients. Specifically, the COFs feature dual active sites—disulfide or diselenide groups—that are cleaved by ROS, facilitating the release of Zn(II) ions with antibacterial and tissue-repairing functions. Additionally, the

Zn(II)-porphyrin COFs demonstrate GOx-like activity, catalyzing the conversion of glucose into non-glucose metabolites. This synergistic mechanism of glucose-responsive Zn(II) release and GOx-like activity helps restore the redox balance in tissues and improves the wound microenvironment, and provides a strategy for diabetic wound healing (Fig. 5d).[114] The innovative design of hydrogels for healing diabetic wounds addresses key pathological barriers such as oxidative stress, inflammation, and poor vascularization through multifunctional platforms. Incorporating immunomodulatory agents, photothermal elements, exosomes, and glucose-regulating components, these hydrogels significantly enhance tissue regeneration and promote angiogenesis. Together, these strategies hold strong

translational potential for effective, personalized diabetic wound care.

3.3. Hydrogels for deep and burn wounds

The increasing prevalence of deep and burn wounds poses a substantial challenge for global healthcare systems, both economically and socially. Traditional wound dressings offer limited support in managing the intricate healing requirements of these severe injuries. Hydrogels have emerged as advanced wound care materials due to their ability to maintain a moist environment and support cellular activities. Their unique properties make them well-suited for promoting effective tissue repair in deep and burn wound management.[115,116] Nazemoroaia and colleagues developed a human skin-like asymmetric wound dressing in 2025. The dressing has a chitosan and alginate hydrogel bottom and an electrospun PCL–silk sericin (PCL-SS) top layer. The inner layer contains queen bee acid (10-HDA), an anti-inflammatory, antibacterial, and immunomodulatory compound, to boost its therapeutic benefits. The dressing was extensively tested *in vitro* and *in vivo* to prove its wound-treatment efficacy. The top layer protected against infection and physical injury, while the hydrogel layer sped up wound healing. Incorporating 1% 10-HDA into the dressing enhanced both cell proliferation and antibacterial activity. In Wistar rats, the 10-HDA-enriched dressing accelerated wound healing without inducing inflammatory adverse effects.[117] The formation of hydrogels for wound dressing involves integrating various materials with unique properties. Graviola fruit extract (GrE) enhances anti-inflammatory, antimicrobial, and antioxidant properties, contributing to accelerated wound healing. Furthermore, in this research, the freeze–thaw technique was used to synthesize composite hydrogels composed of polyvinyl alcohol (PVA) and hyaluronic acid (HA), cross-linked with glutaraldehyde and infused with GrE. This study examined multiple characteristics of the hydrogels, such as swelling capacity, porosity, gel fraction, and morphology. The findings revealed that the incorporation of GrE influenced the physicochemical properties of the hydrogels. The hydrogels exhibited excellent absorption of wound exudate, with an increase in porosity corresponding to higher levels of GrE. The results confirmed that GrE-enriched hydrogels (designated as Gr1 and Gr2) demonstrated superior hemolytic, hemostatic, antibacterial, and wound healing capabilities.[118] Biopolymer hydrogels offer unique properties that support tissue repair by providing a hydrated and protective environment. Dawood *et al.* developed chitosan/fibroin hydrogels incorporated into PVP and cross-linked with 3-aminopropyl(diethoxy)methylsilane (APDEMS) to enhance wound healing. Wound healing studies showed that the fibroin-rich hydrogels achieved a remarkable wound reduction rate of 99.06%, significantly outperforming the control group, which achieved a 67.03% reduction. Histological analysis confirmed these findings, revealing dense fibrous connective tissue in the fibroin-treated group compared to controls. This research provides compelling preclinical evidence that chitosan–fibroin hydrogels enhance angiogenesis in developing chicks and accelerate wound healing in mice, with no apparent toxicity.[119] A new reversibly adhesive hydrogel has been developed for oral wound treatment, addressing the challenge of strong adhesion and easy removal. The hydrogel is created through free radical copolymerization of the cationic monomer [2-(acryloyloxy)ethyl] trimethylammonium chloride (ATAC), the hydrophobic monomer glycol phenyl ether acrylate (PEA), and *N*-isopropylacrylamide (NIPAAm). The cationic salts enable electrostatic interactions, while hydrophobic and PNIPAAm segments provide additional bonding and hydrogen bonding. The hydrogel adheres strongly to oral mucosa (18.67 kPa) and can seal wounds in 10 s. With a lower critical solution temperature of 40.3 °C, it is easily removed with water. It also demonstrates excellent anti-swelling and antibacterial properties, as well as reducing inflammation and supporting tissue regeneration in animal models. This hydrogel shows great promise for managing oral wounds.[120] Huang aimed to explore the impact of an adhesive, conductive hydrogel as a therapeutic dressing on wound healing. A PVA/QCS/TP@Fe^{3+} hydrogel (PQTF) dressing was developed using a straightforward one-pot synthesis combined with the freeze–thaw technique. The hydrogel incorporates PVA, CS quaternary ammonium salt (QCS), tea polyphenols (TP), and Fe^{3+}. Due to its exceptional swelling property, adhesion, and electrical conductivity, the $PQTF_{600}$ hydrogel enhanced the healing process of wounds in an *in vivo* model (Fig. 6a).[121] In a 2024 study, a CS, gallic acid (GA) and cysteine (Cys) hydrogel was developed, referred to as CCG hydrogel, with antioxidant and antibacterial properties. The CCG hydrogel exhibited strong antibacterial effects and good compatibility with blood *in vitro* analysis. In the *in vivo* phase, the hydrogel promoted wound healing, enhanced angiogenesis, supported collagen formation, and upregulated the expression of anti-inflammatory factors.[122] In another study, an oxidized soybean cellulose nanocrystal with PAM hydrogel (CNCs/PAM) was developed. The formulation of the CNCs, crosslinkers, and water in the system was systematically calibrated to enhance the rheological transparency, properties, and micro-network of the CNCs/PAM hydrogel. This study also explored the hydrogel's potential for use in wound dressing applications.[123] Other work reported a dextran-based HA hydrogel (DA-AHA) by combining aminated hyaluronic acid (AHA) and aldehyde-modified dextran *via* a Schiff base reaction. The hydrogels exhibited rapid blood coagulation within 60 s and significantly enhanced wound healing in animal models. Additionally, the influence of molecular weight on the structural stability and wound-healing efficiency of dextran–AHA hydrogels was thoroughly examined, confirming their potential for enhancing acute inflammation repair and wound closure (Fig. 6b).[124] Glycyrrhetinic acid-based supramolecular nanofiber hydrogel has emerged as a promising material for wound healing due to its excellent mechanical stability, low swelling ratio, and pro-angiogenic properties This hydrogel is consists of a self-assembled glycyrrhetinic acid nanofibrous structure integrated with a cross-linked GG network. Moreover, *in vitro* and *in vivo* experiments validated its biocompatibility and notable pro-angiogenic properties, and the
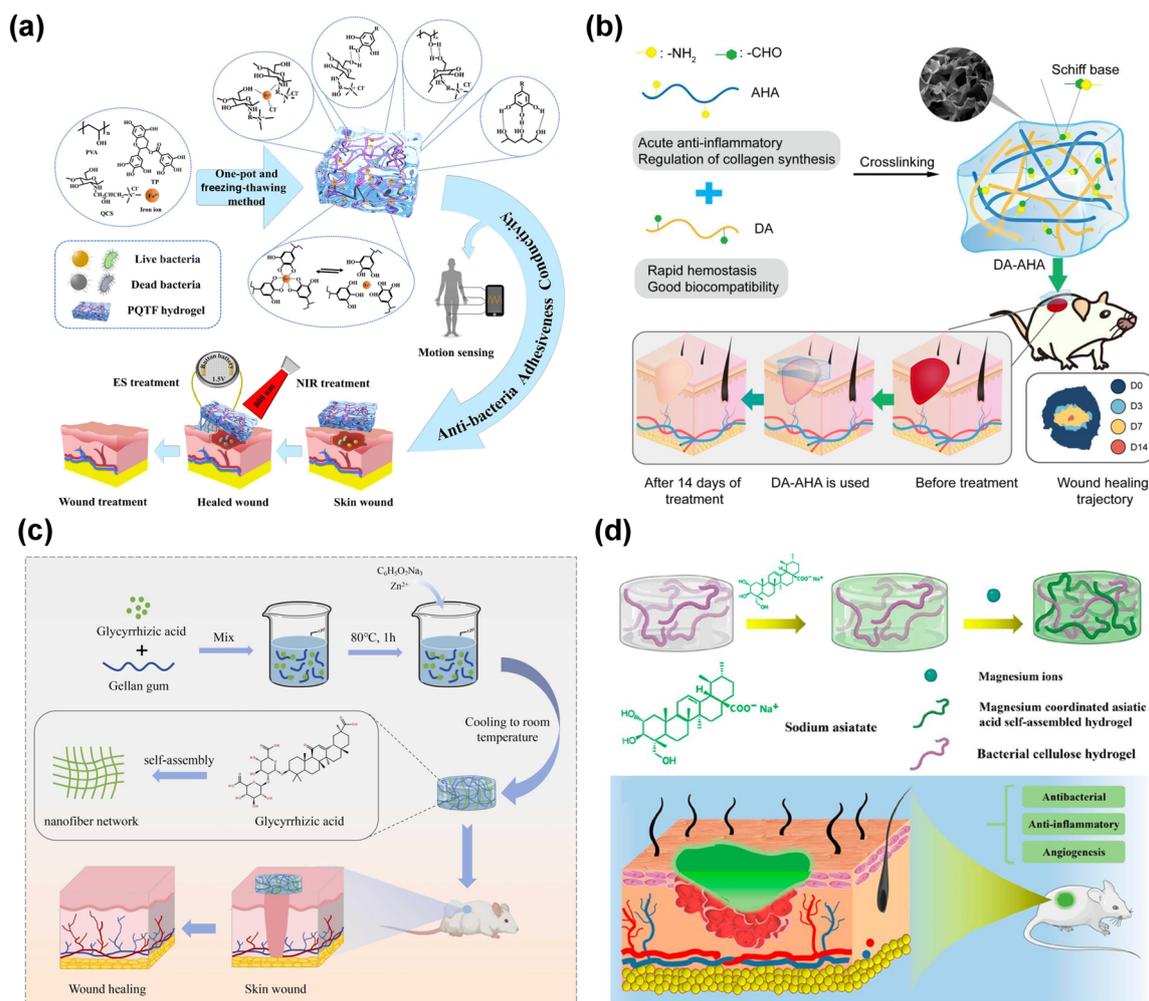
Fig. 6 (a) Representation of the development of an adhesive conductive hydrogel dressing intended for integrated electrical stimulation and PTT aimed at improving chronic wound healing. Reproduced with permission from ref. 121. Copyright 2025 Elsevier. (b) Illustrative depiction of the synthesis procedure for a range of dextran-based DA-AHA hydrogels intended for application in dressings for wound healing. Reproduced with permission from ref. 124. Copyright 2024 Elsevier. (c) Schematic image of a supramolecular nanofiber network hydrogel and its application on skin wounds. Reproduced with permission from ref. 125. Copyright 2025 Elsevier. (d) Schematic illustration outlining the preparation and therapeutic mechanisms of the AA-Mg/BC hybrid hydrogel dressing, emphasizing its anti-inflammatory, antibacterial, and angiogenic effects. Reproduced with permission from ref. 132. Copyright 2024 American Chemical Society.

animal wound model GG/glycyrrhetinic acid hydrogel achieved a 95.49 ± 1.1% wound healing rate within 14 days (Fig. 6c).[125] Another study explored gallium maltolate (GaM) as an antimicrobial agent loaded hydrogel gauze. The GaM-loaded hydrogel demonstrated strong antibacterial properties, making it a promising solution for chronic wound treatment. In an equine wound model, the hydrogel foam dressing demonstrated its potential to fight MRSA infection and support chronic wound healing with controlled GaM release.[126] In 2024, Wang et al. developed advanced multifunctional hydrogels by combining fibrin with *Bletilla striata* polysaccharides (BSPs) or oxidized *Bletilla striata* polysaccharides (OBSPs), aiming to create effective wound dressings.[127] A hybrid hydrogel, TA-GL/OSA/ZnO, was developed in this study using a double-network cross-linking method. The hydrogel is composed of Gel, TA, OSA, and ZnO NPs. The combined effects of

TA and ZnO NPs resulted in the composite hydrogels exhibiting robust antibacterial activity against *S. aureus* (97.8% ± 0.9%) and *E. coli* (96.6% ± 1.2%), as well as enhanced mechanical properties. Overall, this multifunctional hydrogel showed significant potential for wound healing therapy and wide application in medical treatments.[128] Wang and colleagues developed an innovative hydrogel dressing by incorporating silver nanowires (AgNWs) into methacrylated gelatin (GelMA) through mechanical blending and UV light curing. The inclusion of AgNWs enhanced the hydrogel's mechanical properties and imparted electrical conductivity. This hydrogel dressing shows promise for applications in monitoring changes to wound conditions.[129] A novel zwitterionic polymer hydrogel (LST) was created for the purpose of serving as functional wound dressings. The hydrogel is composed of a zwitterionic monomer ([2-(methacryloyloxy)ethyl]dimethyl-(3-sulfo-

propyl) ammonium hydroxide), with mussel-inspired THMA (*N*-[tris(hydroxymethyl)methyl]acrylamide) and lithium magnesium salt. This hydrogel was able to adhere to the skin effectively due to the outstanding adhesion properties of the THMA monomer, which contained three hydroxyl groups (~6.0 kPa). This adhesion not only safeguards the incision and improves therapeutic outcomes, but also enables painless removal, thereby reducing patient distress. The hydrogel was endowed with potent antimicrobial and mechanical properties by the zwitterionic sulfobetaine units of the SBMA.[130] Huang *et al.* created a tunable, versatile anti-inflammatory hydrogel platform that was derived from sulfated alginates (Algs) and enriched with PB nanozymes. This platform effectively eliminates excess ROS from the wound environment.[131] Asiatic acid (AA), a compound extracted from herbs, is well-known for its strong anti-inflammatory, antibacterial, and angiogenic properties, making it an ideal candidate for integration into hydrogel carriers for wound healing applications. A new hybrid hydrogel dressing has been developed, featuring interpenetrating polymer networks formed by self-assembled AA coordinated with magnesium ions with bacterial cellulose (BC), to enhance the healing of infected chronic wounds (Fig. 6d).[132] In 2024, An and colleagues introduced an upconversion-photopolymerization-driven approach, developing injectable UC-YT@NY + GelMa hydrogel hybrids aimed at enhancing *in vivo* wound healing. An 808 nm NIR laser with a power density of 1.27 W cm^{-2} is applied for 8 min and the hydrogel achieves a photopolymerization efficiency of 96.3%. The biocompatible hydrogel promoted effective deep wound healing, achieving full recovery in mouse models within 7 days at a depth of 3 mm. This innovative therapeutic strategy offers precise spatiotemporal control over the release of therapeutic agents, delivering exceptional results in deep-tissue wound healing.[133] A multifunctional hydrogel was synthesized utilizing BC coated with PDA@BC and PVA *via* dynamic borate PB ester bond crosslinking in another investigation. The hydrogels demonstrated improved tissue adhesion, self-repair capacities, and blood-clotting characteristics. The PB-PDA@BC hydrogels, infused with doxycycline hydrochloride (Doxy), exhibited significant antibacterial properties *via* prolonged drug release. Furthermore, the hydrogels exhibited a substantial swelling ratio, exceptional biocompatibility, and adequate mechanical strength. In comparison with standard Tegaderm film dressings, the PB-PDA@BC/Doxy hydrogel dressings markedly enhanced wound healing of full-thickness wounds and were effective in wound dressing applications.[134] Hydrogels offer significant advantages for deep and burn wound management due to their ability to maintain a moist environment, support tissue regeneration, and incorporate therapeutic agents. Recent innovations, ranging from natural bioactive compounds to multifunctional and responsive hydrogel systems, demonstrate strong antibacterial, anti-inflammatory, and regenerative properties in preclinical models. These findings highlight the promising future of hydrogel-based dressings for improving outcomes for severe wound healing (Table 1).

4. Emerging theranostic hydrogels: a foundation for next-generation wound management

Theranostic hydrogels represent a groundbreaking advancement in wound healing by integrating therapeutic and diagnostic functionalities into a single platform. These innovative hydrogels combine the inherent benefits of hydrogels, such as high water content, biocompatibility, and flexibility, with theranostic capabilities, enabling simultaneous treatment and monitoring of wounds. By incorporating therapeutic agents, such as antimicrobial or anti-inflammatory compounds, alongside imaging or sensing elements, theranostic hydrogels provide real-time feedback on wound status, enhancing personalized and efficient care. This dual-functionality not only improves the healing process but also allows for the continuous assessment of the wound environment, paving the way for more targeted and responsive treatments.

4.1. Theranostic hydrogels for diabetic wounds

Diabetic wounds are chronic and complex injuries that exhibit delayed healing due to factors such as impaired circulation, persistent inflammation, and peripheral neuropathy. These wounds can occur in various parts of the body and are often resistant to conventional treatments, which typically address only isolated aspects of the wound-healing process. Theranostic hydrogels offer a promising alternative by combining therapeutic and diagnostic capabilities in a single platform. These advanced materials respond to the wound environment, enabling more effective, targeted, and timely healing in diabetic patients.[135,136] Chronic wounds, particularly those associated with diabetes, present a significant public health challenge and impose considerable economic burdens. This work explores a novel solution: a wireless theranostic patch designed for real-time monitoring and targeted treatment to enhance wound healing. The patch integrates cutting-edge materials that are multifunctional and electro-responsive, combining smart hydrogels with wearable bioelectronics to revolutionize diabetic wound care. These materials enable continuous monitoring of glucose and pH levels, facilitating precise, personalized treatments such as insulin delivery through iontophoresis and electrical stimulation. A smart multifunctional hydrogel, known as MFCPH, is created by embedding PDA-doped polypyrrole (PPy) (PDAPPy) nanofibrils within a PAM matrix through an *in situ* formation process. This unique structure, along with the polycationic backbone of the PDA-PPy nanofibrils, imparts the hydrogel with exceptional drug-loading capacity, light transparency, skin adhesion, electrical conductivity, and broad-spectrum antimicrobial properties. When loaded with insulin, MFCPH works in tandem with iontophoretic electrodes to enable on-demand drug delivery and electrical stimulation. The Therapatch's adhesive design, combined with the flexibility of polyethylene terephthalate (PET), provides robust resistance to physical deformation. This innovative wireless theranostic patch represents a promising advancement in

Table 1 Multifunctional hydrogel composites: biological assessments and wound healing outcomes

Hydrogel composite	Bacterial strains (antibacterial testing)	In vitro biocompatibility (cell lines)	In vivo model (animal studies)	Therapeutic effects	Ref.
Bacterial wounds					
MXene-Ag-PDA-(PNVAO)/M-A-P	E. coli, MRSA	L929 cells	Female Kunming mice (MRSA)	Anti-bacterial, antioxidant, wound healing	78
OSD/CMC/Fe/PA hydrogel	E. coli, MRSA	L929 cells	Female Kunming mice (MRSA)	Anti-bacterial, antioxidant, hemostatic, wound healing	79
CEC/PF/CNT2	E. coli, S. aureus	L929 cells	Female Kunming mice (S. aureus)	Anti-bacterial, hemostatic, wound healing	80
PBEC	E. coli, P. aeruginosa, S. aureus, C. albicans	L929 cells	Male Kunming mice (S. aureus)	Anti-bacterial, hemostatic, antioxidant, wound healing	81
UPy-PEGSDU-CuS NPs	E. coli, MRSA	L929 cells, HUVEC cells	Female Kunming mice (MRSA)	Anti-bacterial, antioxidant, angiogenesis, wound healing	82
PVA/chitosan/PDA	E. coli, S. aureus	L929 cells		Anti-bacterial, wound healing	83
CEC-OHA-NDs	E. coli, S. aureus	L929 cells	Female Balb/c mice (S. aureus)	Anti-bacterial, hemostatic, anti-inflammatory, wound healing	84
HA-PT/HUOH	E. coli, S. aureus	HSF, L929 cells, RAW264.7 cells, HUVEC cells	Balb/c mice (S. aureus)	Anti-bacterial, hemostatic, anti-inflammatory, antioxidant, wound healing	85
GelMA/MOF	E. coli, S. aureus	L929 cells	Balb/c mice (E. coli and S. epidermidis)	Anti-bacterial	86
DTTPB@gel	E. coli, S. epidermidis	NIH3T3 cells, HUVEC cells		Anti-bacterial, wound healing	87
KGM/PAM/Ga^{3+}	E. coli, S. aureus	L929 cells	Male Kunming mice (S. aureus)	Anti-bacterial, wound healing	88
HAQ-Hal-Ag-F	E. coli, S. aureus	NIH3T3 cells		Anti-bacterial	89
Rif@GelMA-NBNAGA/LAP	E. coli, S. aureus	L929 cells	Male Balb/c mice (S. aureus)	Anti-bacterial, wound healing	90
PDA-PTA-Cur 16	S. aureus	L929 cells	SD rats (S. aureus)	Anti-bacterial, antioxidant, wound healing	91
SNP@PCN@Gel	E. coli, S. aureus	HUVEC cells	Balb/c mice (S. aureus)	Anti-bacterial, angiogenesis, wound healing	92
Jelleine-1	S. aureus, MRSA, E. coli, and C. albicans	NIH3T3 cells	Male Balb/c mice (MRSA)	Anti-bacterial, wound healing	93
PNVBA	E. coli, MRSA	L929 cells		Anti-bacterial	94
L5@LysSYL	S. aureus, MRSA, A. baumannii, P. aeruginosa, E. coli	HaCaT cells	Female, Balb/c mice (S. aureus)	Anti-bacterial, anti-inflammatory, wound healing	95
CPO-Alg	E. coli, S. aureus		Female Kunming mice (S. aureus)	Anti-bacterial, wound healing	96
P/A/AB/M	P. aeruginosa, MRSA	L929 cells	Female Kunming mice (P. aeruginosa)	Anti-bacterial, wound healing	97
CSL/SA	E. coli, S. aureus	L929 cells		Anti-bacterial, antioxidant	98
PAcN/Ag@Clay-TA	E. coli, MRSA	L929 cells	Balb/c mice (MRSA)	Anti-bacterial, antioxidant, anti-inflammatory, angiogenesis, wound healing	99
nanoAg@QAC	E. coli, S. aureus	HUVEC cells	Male Goto-Kakizaki rats (P. aeruginosa and S. aureus)	Anti-bacterial, anti-inflammatory, angiogenesis, wound healing	100
GG@Gel-Ca	E. coli, S. aureus	L929 cells	Rat (S. aureus)	Anti-bacterial, hemostatic, wound healing	101
PVA/chitosan/Cu NWs	E. coli, S. aureus	HDF cells	C57/BL6j mice (S. aureus)	Anti-bacterial, wound healing	102
TSNH	S. aureus, E. coli, MRSA	L929 cells	Wistar rat (S. aureus)	Anti-bacterial, anti-inflammatory, angiogenesis	103
CGrAP	S. aureus	L929 cells		Anti-bacterial, wound healing	104
Diabetic wounds					
BSA-CLP	E. coli, S. aureus	NIH-3T3 cells, HaCat cells	Adult zebrafish, male Balb/c mice	Anti-bacterial, wound healing	106
Collagen-polyurethane-dextran		RAW 264.7 cells	Male Wistar rats, adult male rabbits	Anti-inflammatory, wound healing	107
Se-Tz	E. coli, MRSA	NIH-3T3 cells, HUVEC cells	Male ICR mice	Anti-inflammatory, Anti-bacterial, Antioxidant, wound healing	108

Table 1 *(Contd.)*

Hydrogel composite	Bacterial strains (antibacterial testing)	In vitro biocompatibility (cell lines)	In vivo model (animal studies)	Therapeutic effects	Ref.
QHT@PBNPs		L929 cells	Male Sprague-Dawley (SD) rats	Immunoregulation, proangiogenesis, hemostatic, wound healing	109
DMM/GelMA		RAW264.7 cells	C57BL/6 mice	Anti-inflammatory, wound healing	110
HGAS	E. coli, S. aureus	NIH-3T3 cells	SD male rats	Anti-bacterial, Angiogenesis, anti-inflammatory, wound healing	111
AC-hydrogel	E. coli, P. aeruginosa, S. aureus		Male Wistar rodents	Anti-bacterial, wound healing	112
Q5Exo			Adult Lepr db/dP diabetic mice	wound healing	113
Deep and burn wounds					
PCL-SS-CS-Alg (10-HDA)	E. coli, S. aureus	NIH3T3 cells	Male Wistar rat	Anti-inflammatory, anti-bacterial, immunomodulatory, wound healing	117
GrE-PVA-HA	E. coli, K. pneumonia, S. aureus, B. subtilis		Swiss Albino female mice	Anti-bacterial, anti-inflammatory, antioxidant, hemostatic, wound healing	118
Chitosan/fibroin biopolymer			Male albino Swiss Webster mice	Angiogenesis, wound healing	119
PAPN	E. coli, S. aureus, S. mutans	RGF cells	Male rats	Anti-bacterial, wound healing	120
PQTF	S. aureus, E. coli, MRSA, P. putida	L929 cells	ICR mice	Anti-bacterial, hemostatic, antioxidant, wound healing	121
CCG	E. coli, S. aureus		9 SPF-grade female mice	Anti-bacterial, antioxidant, hemostatic, wound healing	122
CNCs/PAM	E. coli, S. aureus	L929 cells	SD rats	Anti-bacterial	123
DA-AHA		L929 cells	Female SD rats	Hemostatic, wound healing	124
GG/GA		HUVECs	SD rats	Wound healing	125
GaM-loaded PLGA microspheres	MSSA, MRSA	hDF cells	Equine distal limb wound model	Anti-bacterial, wound healing	126
Fibrin-OBSP	E. coli and S. aureus		Male Kunming mice	Anti-bacterial, antioxidant, anti-inflammatory, wound healing	127
TA-GL/OSA/ZnO	E. coli, S. aureus	NIH3T3 cells	Balb/c mice	Anti-bacterial, antioxidant, wound healing	128
GMAN	E. coli, S. aureus	L929 cells	Rat	Anti-bacterial, hemostatic, wound healing	129
LST zwitterion	S. aureus, E. coli, and C. albicans	NIH3T3 cells, L929 cells, HUVEC cells, and RSC96 cells	Male SD rats, Female Balb/c mice	Anti-bacterial, hemostatic, wound healing	130
PB@Algs-H		HUVECs cells, NIH3T3 cells, Raw264.7 cells	Male C57 mice	Anti-inflammatory, antioxidant, wound healing	131
AA-Mg/BC	E. coli, S. aureus	HUVEC cells, THP-1 cells	Male Balb/c mice	Anti-bacterial, anti-inflammatory, angiogenesis, wound healing	132
UC-YT@NY + GelMa		L929 cell	SD rats, Balb/c mice	wound healing	133

personalized healthcare, focusing on real-time, patient-specific care for chronic wounds through advanced material integration and electro-regulated therapies (Fig. 7a–e).[137] Yang and colleagues developed modular hydrogels capable of monitoring key physiological markers in diabetic wounds, including pH, glucose levels, and temperature. Glucose detection was enabled by incorporating photonic crystal (PC) structures within glucose-responsive hydrogels. These PC hydrogels (PCHs) enabled visual glucose level monitoring within physiological ranges by displaying distinct structural color changes in response to glucose-induced swelling or contraction. The hydrogels also featured pH sensing through embedded acid–base indicator dyes and temperature detection using thermochromic powders. These multifunctional hydrogels successfully monitored real-time physiological changes during diabetic wound healing in both *in vitro* and *in vivo* experiments, providing a valuable tool for biomarker-based wound management and treatment (Fig. 7f).[138] In another report, hydrogels composed of quaternary carboxymethyl chitosan (QCMCS) and oxidized sodium alginate (OSA) were engineered by encapsulating glucose oxidase (GOx) and gold nanoclusters (AuNCs), followed by immersion in a tannic acid (TA) solution to impart multifunctional therapeutic and diagnostic properties. This formulation offered antibacterial, antioxidant, pro-angiogenesis, and pro-collagen deposition properties, along with real-time monitoring capabilities. Additionally, these hydrogels enabled the real-time collection of image signals, allowing for accurate monitoring of glucose levels in diabetic wounds and providing timely insights into the wound healing process. The findings highlight TA-QCMCS/OSA@GOx@AuNC hydrogels as an innovative approach for the real-time monitoring and treatment of diabetic wounds.[139] A theranostic hydrogel dressing incorporating a boron-based probe was developed for monitoring and the tailored healing of chronic wounds. The boron-based probe is formed by the interaction between borax (B) and TA, serving as a cross-linker in the creation of guar gum/PVA/BT (GPBT) hydrogels. These hydrogels enable visual monitoring through color changes, providing an easy way to track wound conditions. Additionally, they support remote diagnostics by connecting with a smartphone interface for convenient health management while adapting to various stages of chronic wound healing.[140] The development of CS hydrogels with polymerized ionic liquids and a NIR fluorescent probe (PIL-CS) offers a promising wound healing approach. This method helps prevent acute wounds from becoming chronic and enables the real-time monitoring of wound microenvironments (Fig. 7g).[141] Theranostic hydrogels represent a transformative approach for managing diabetic wounds by integrating therapeutic and diagnostic functions into a single platform. These smart systems enable the real-time monitoring of key biomarkers like glucose, pH, and temperature, while offering targeted treatments such as insulin delivery, antimicrobial action, and tissue regeneration. Innovations like wireless patches, photonic crystal-based sensors, and multifunctional nanocomposites demonstrate the potential of these hydrogels to significantly enhance personalized wound care.

4.2. Theranostic hydrogels for bacterial wounds

Bacterial wounds present a major clinical challenge due to the risk of severe infection, delayed healing, and potential complications. Traditional diagnostic methods are slow and invasive, limiting timely and effective treatment. Theranostic hydrogels offer a smart approach by combining infection sensing with localized therapy. This integrated strategy enables real-time monitoring and targeted intervention for improved bacterial wound management.[142] Yang *et al.* developed a photopolymerized hydrogel dressing for wound care and vital sign monitoring in cold environments. The dressing features an interpenetrating network (IPN) structure formed with BC, enhancing water retention and mechanical strength (540.37 kPa), while maintaining resilience and electrical conductivity (9.01×10^{-3} S cm^{-1}) at temperatures as low as -20 °C. QAS imparts strong antibacterial properties by disrupting the membranes of *S. aureus* and *E. coli*, causing intracellular fluid leakage. In rat-infected wound models, the hydrogel demonstrated reduced inflammation, faster healing, and accelerated recovery, as confirmed by H&E staining. Additionally, the hydrogel serves as an electrode for monitoring electrocardiogram (ECG) signals and respiratory status, enabling real-time vital sign tracking. This multifunctional dressing holds significant potential for wound treatment and physiological monitoring in cold outdoor environments (Fig. 8a).[143] For smart pH monitoring and wound infection prevention, Zou *et al.* created a theranostic hydrogel system using dual-site biomimetic FeNi MOFs. The FeNi-MOFs provide excellent stability by simulating the actions of three enzymes: peroxidase (POD), superoxide dismutase (SOD), and catalase (CAT). These MOF-infused hydrogels act as wound dressings, supporting healing and enabling the precise tracking of wound conditions (Fig. 8b).[144] Theranostic antibacterial wound dressings offer multifunctional benefits for practical applications. In 2024, Zhang *et al.* developed a pH- and light-responsive hydrogel using PVA and polyaniline (PANi), cross-linked with phytic acid (PA) derived from rice bran. This conductive hydrogel enables *in situ* infection detection and photothermal sterilization, promoting wound healing. The pH sensitivity of PANi detects bacterial infections at concentrations as low as 10^3 CFU mL^{-1}, while NIR absorption triggers localized heating, achieving nearly 100% bacterial eradication (*S. aureus* and *E. coli*) under 808 nm NIR laser irradiation for 20 min. The hydrogel also monitors joint movements, reducing the risk of wound re-opening. *In vitro* and *in vivo* evaluations confirmed its excellent biocompatibility, strong antibacterial efficacy, and ability to accelerate healing in infected wounds. This innovative hydrogel holds promise for advancing wearable devices and precision medicine.[145] Injectable theranostic hydrogels were designed for the long-term visual monitoring of infected wounds and antibacterial effects without antibiotics. This hydrogel, synthesized from ε-polylysine (ePL), was formed by copolymerizing methacrylated ePL (mPL) with tetrakis(4-carboxyphenyl) porphyrin (mPL-TCPP) and phenol red (mPL-Pr). Upon light exposure, mPL-TCPP generates ROS, enabling free radical crosslinking to
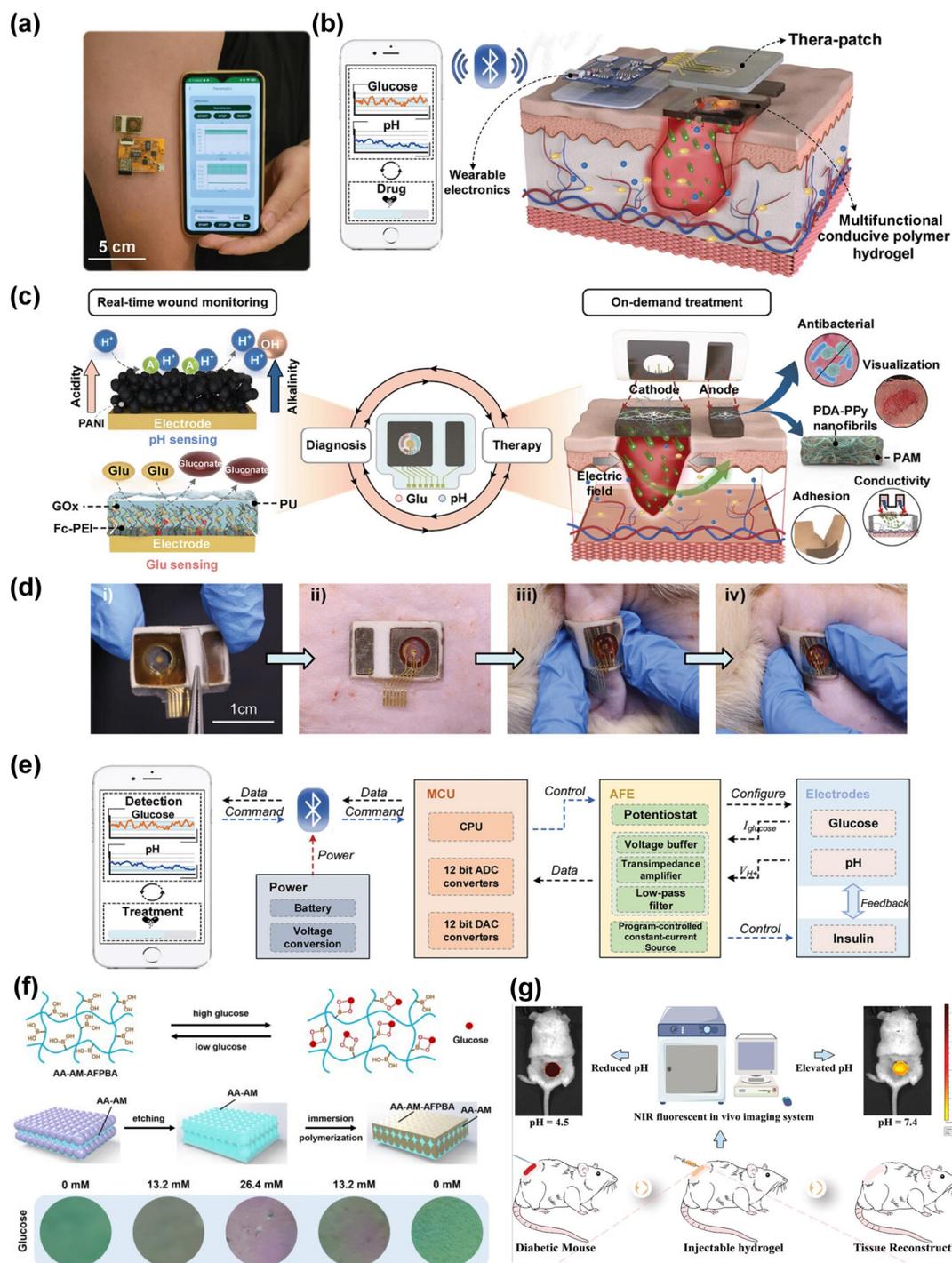
Fig. 7 (a) A wireless theranostic system designed for diabetic wound management is depicted and the photograph showcases the fully integrated wireless system for diabetic wound care. (b) Schematic illustration outlining the components of the wireless theranostic system, which includes a customized smartphone application, a wearable electronic device, and the Thera-patch. The Thera-patch facilitates continuous wound monitoring and delivers targeted treatment by integrating iontophoresis with the multifunctional hydrogel (MFCPH). The wearable device gathers sensing data and processes commands from the app to initiate drug delivery. The smartphone app analyzes the wound condition from received data and sends commands for drug administration. (c) The system employs a closed-loop strategy for real-time wound monitoring and on-demand treatment. (d) The Thera-patch application involves two steps: (i) removing the sealing membrane, and (ii) applying the Thera-patch to the diabetic rat's wound. The patch's mechanical properties are demonstrated through (iii) bending and (iv) twisting. (e) A block diagram illustrating the wireless wound thera-nostic system, showing the command and data flow for continuous monitoring and targeted drug delivery. Reproduced with permission from ref. 137. Copyright 2024 Wiley. (f) Schematic representation of the synthesis process and glucose-responsive mechanism of photonic crystal hydrogels (PCHs). Reproduced with permission from ref. 138. Copyright 2024 Springer Nature. (g) Schematic of NIR fluorescent hydrogel PIL-CS for real-time imaging in diabetic mice. Reproduced with permission from ref. 141. Copyright 2023 Wiley.
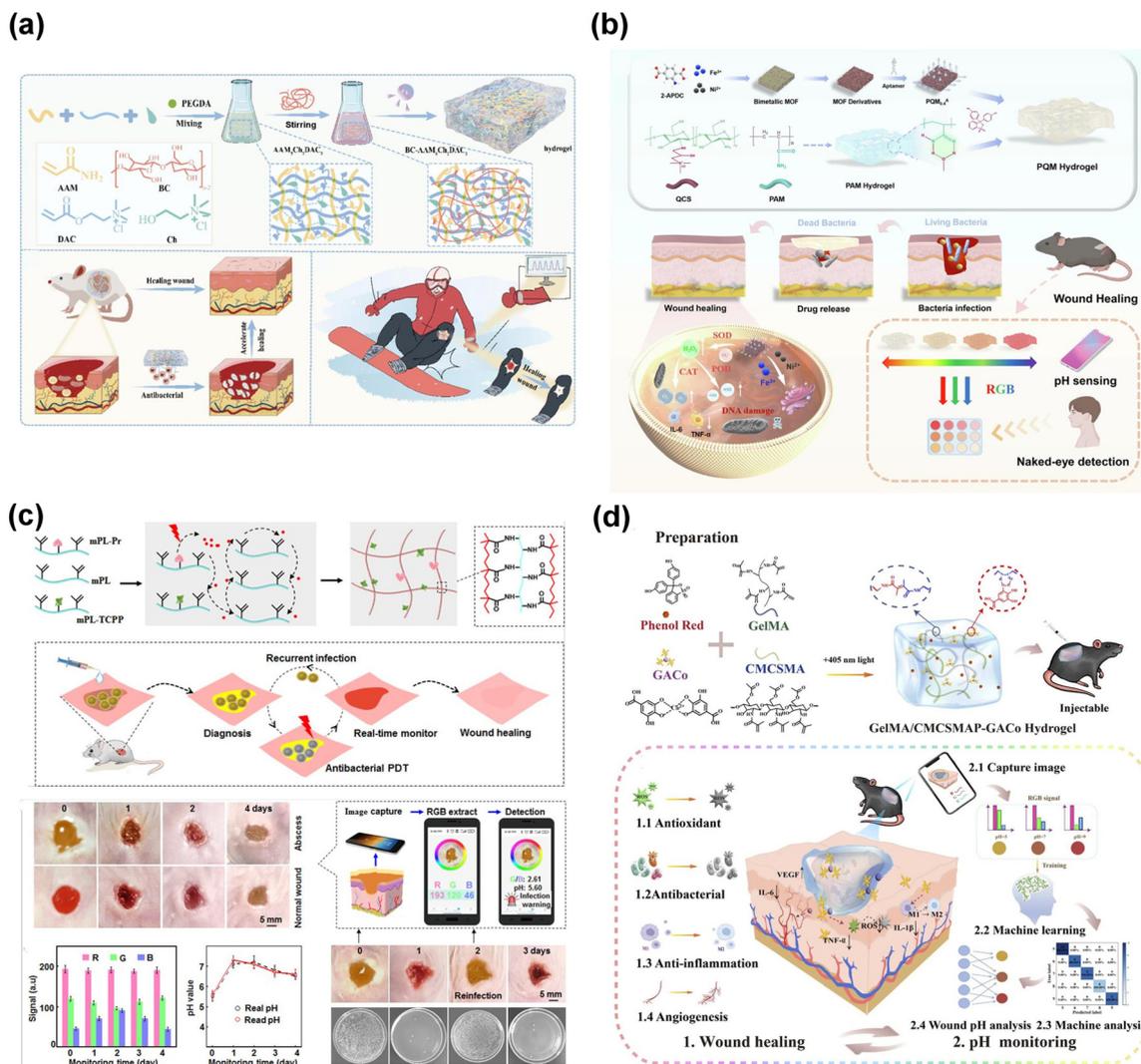
Fig. 8 (a) Illustration depicting the preparation process for the BC-AAM5Ch2DAC3 hydrogel and its role in accelerating wound healing and monitoring. Reproduced with permission from ref. 143. Copyright 2024 Elsevier. (b) Schematic illustration of FeNi-MOF-based theranostic hydrogels developed for wound assessment and therapy. Reproduced with permission from ref. 144. Copyright 2024 Elsevier. (c) Schematic of PL@Pr-TCPP hydrogel synthesis, theranostic mechanism, *in vivo* sensing of bacterial infection, and infection recurrence monitoring. Reproduced with permission from ref. 146. Copyright 2024 Elsevier. (d) Schematic representation of the synthesis procedure for GelMA/CMCSMAP-GACo hydrogel. Diagram illustrating the potential application mechanism of the hydrogel in the promotion of wound healing. Reproduced with permission from ref. 147. Copyright 2024 Elsevier.

form PL@Pr-TCPP hydrogels without photoinitiators while simultaneously delivering antibacterial PDT. This hydrogel undergoes rapid pH-dependent color changes, transitioning from yellow to orange to red (pH 5.0 to 9.0), allowing bacterial levels to be evaluated through smartphone-based green-to-blue (G/B) signal ratios. The integration of phenol red and TCPP enhances bacterial infection diagnosis and provides a sustained antibacterial effect with repeated light exposure. The ePL hydrogels' ability to capture bacteria further enhances the PDT effect by mitigating the short lifespan and limited range of ROS. This study introduced an effective strategy for developing theranostic hydrogel dressings capable of lifecycle diagnosis and on-demand treatment of wound care (Fig. 8c).[146] A

similar report, monitoring pH levels in wounds, can act as an early indicator of infection risk, aiding in improved wound care by tracking pH fluctuations. This study developed a smart hydrogel for wound care, incorporating machine learning-assisted analysis for enhanced management. The hydrogel was composed of a GelMA and CMCSMA (double cross-linked network), integrated with cobalt-GA-based metal-phenolic NPs (GACo MPNs) for enhanced therapeutic action. Phenol red was incorporated as a pH indicator, allowing for the real-time monitoring of wound conditions. The hydrogel exhibited remarkable injectability and shape adaptability, ensuring easy application to irregular wound surfaces. The hydrogel's unique pH-responsive color changes allowed for real-time wound

monitoring, with image analysis facilitated through smartphone integration and machine learning algorithms. This innovative approach offers a comprehensive solution for improving diabetic wound healing and care (Fig. 8d).[147] The antimicrobial peptide εePL and PDA NPs were used to create injectable theranostic hydrogels for targeted bacterial debris removal, imaging-guided antibacterial PDT, and real-time infection detection. ePL was conjugated with ureido-pyrimidinone to form PLU hydrogels through quadruple hydrogen bonding, while PDA NPs loaded with tetrakis(4-carboxyphenyl) porphyrin (TCPP) (PTc) were incorporated, creating Schiff base linkages within the PLU@PTc hydrogels. This approach showcases a practical strategy for theranostic wound management through infection-triggered visual diagnostics, effective non-antibiotic sterilization, and on-demand hydrogel removal with bacterial debris clearance.[148] Theranostic hydrogels for bacterial wounds enable real-time infection detection and targeted, often non-antibiotic, therapy. These smart systems significantly enhance wound healing through integrated diagnostics and responsive treatment.

4.3. Theranostic hydrogels for skin wounds

Burns and skin wounds often lead to inflammation, infection, and delayed healing, presenting serious clinical challenges. Theranostic hydrogels provide a multifunctional platform that combines targeted therapy with real-time monitoring of wound conditions. Their ability to conform to wound sites and deliver antimicrobial agents enhances healing while reducing infection risk. These smart materials represent a significant advancement in the treatment of complex epidermal injuries.[149] In 2025, a pH-sensitive and removable wound dressing was developed using the dual functionality of *Brassica oleracea* (red cabbage) extract (RCE) for its pH sensitivity and biological activity. The dressing consisted of two hydrogel types, one made from CS and the other from hydroxyethyl cellulose (HEC), both enriched with RCE to enhance the wound healing properties. These dressings displayed a distinct color change in response to pH variations during wound treatment. The CS/RCE dressing achieved an impressive 99.69% wound closure. RCE contributed significantly to the healing process through its anti-inflammatory, antioxidant, and antimicrobial properties. These dual-function dressings are promising candidates for both sensing and treating skin wounds effectively.[150] A multifunctional hydrogel system was developed using sodium lignosulfonate–AgNPs combined with SBMA. This synergy imparted the hydrogel with strong adhesion, high mechanical strength, and antioxidant and antimicrobial properties. The hydrogel exhibits substantial potential for the development of pressure strain sensors and wound dressings, aiding effective wound healing and enabling limb movement monitoring.[151] A theranostic wound dressing integrating a pH sensor with controlled antibiotic release was developed using silk in 2024. This hydrogel was made with alginate (ALG) and graphene oxide (GO) and incorporated with levofloxacin (LVX) and a pH indicator. When the pH of the epidermis increases, the modified silk undergoes a transformation from yellow to green, signaling the presence of an infection. At higher pH levels, the ionization of carboxyl groups (–COOH) in ALG creates repulsion among carboxylate ions (–COO$^-$), speeding up drug release compared to lower pH conditions. Additionally, these modified silk fibers exhibit antimicrobial properties without causing skin irritation or allergic reactions. This theranostic silk marks a significant advancement in smart wound care.[152] Other research presented a multifunctional eutectogel synthesized from a polymerizable deep eutectic solvent (PDES), formed by a mixture of diallyldimethylammonium chloride (DADMAC), glycerol, polycyclodextrin (PCD), DA-grafted Gel (Gel-DA), and OSA. This eutectogel features reversible Schiff base bonds, hydrogen bonds, and host–guest interactions, allowing it to rapidly self-heal after disruption. The GPDO-15 eutectogel exhibits strong tissue adhesion, impressive stretchability (419%), good ionic conductivity (0.79 mS cm^{-1}), and excellent antibacterial (90%) and self-healing properties. It also shows excellent biocompatibility and can serve as a stable sensor for monitoring human activities. *In vivo* studies confirm its ability to enhance wound healing, positioning it as a promising material for biological dressings (Fig. 9a).[153] A versatile hydrogel sensor was designed and developed utilizing GA-modified CS (CSGA) and 3-carboxyphenylboronic acid-modified CS (CSPBA), including Ag-decorated PDA NPs. The improved sensor, designated Ag@PDA-(CSPBA/CSGA), exhibited a gauge factor of 2.49, a quick response/recovery time of 263 ms, and exceptional endurance. It exhibited self-healing characteristics, antioxidative activity, tissue adhesion, and antibacterial efficacy against *E. coli* (92.76%) and *S. aureus* (98.08%). The hydrogel sensor expedited wound closure and facilitated tissue regeneration as a wound dressing. It was capable of monitoring both fine movements and large-scale motions. This study highlights the potential of this multifunctional epidermal sensor for health monitoring and wound care management (Fig. 9b).[154]

Theranostic hydrogels represent a transformative advancement in biomedical applications, particularly for real-time wound monitoring. By integrating therapeutic and diagnostic functionalities, these hydrogels offer a dual benefit: promoting efficient wound healing while providing continuous, non-invasive monitoring of the healing process. This next-generation technology holds the potential to revolutionize patient care, enabling timely interventions and personalized treatment strategies. As research progresses, the development of more sophisticated and responsive hydrogel systems is expected to further enhance their efficacy and broaden their clinical applications, paving the way for significant improvements in healthcare outcomes (Table 2).

5. Various theranostic wound dressing materials

Theranostic wound dressings integrate therapeutic and diagnostic functions into a single platform, enabling real-time monitoring and targeted treatment of wounds. These
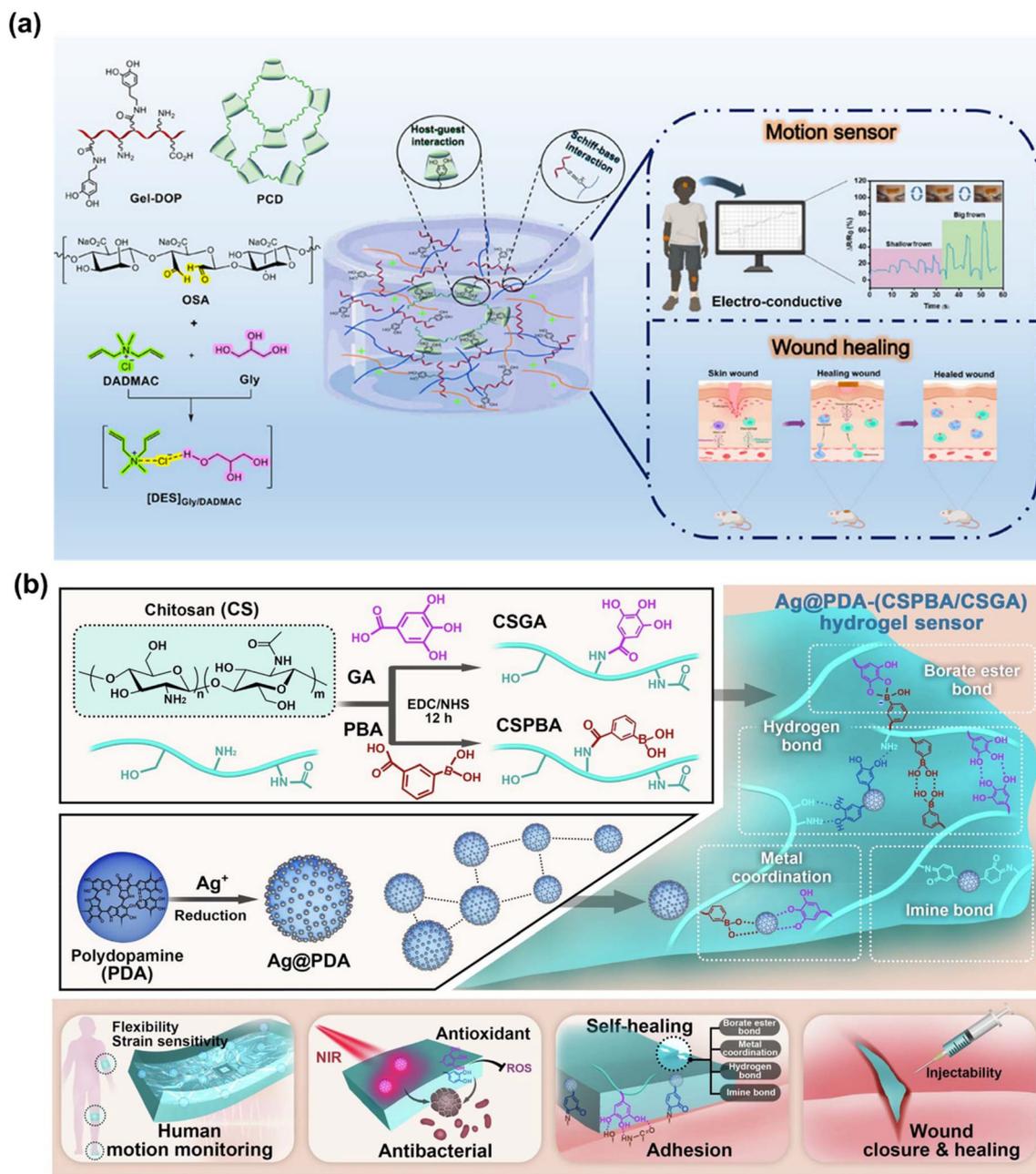
Fig. 9 (a) The electrically conductive, self-healing, adhesive, and antibacterial eutectogel, which is designed for applications in sensing and wound healing, is illustrated. Reproduced with permission from ref. 153. Copyright 2024 American Chemical Society. (b) Schematic representation of the Ag@PDA-(CSPBA/CSGA) hydrogel developed for application in wearable epidermal sensors. Reproduced with permission from ref. 154. Copyright 2024 Springer Nature.

advanced materials offer a smart solution for enhancing healing outcomes and personalized care. Yang *et al.* created a multifunctional wound dressing that integrated europium-doped bioactive glass (EuBG) and MoO_{3-x} nanosheets inside a sodium alginate matrix (MoO_{3-x}-EuBG-SA) to improve diabetic wound healing and monitoring. The dressing was engineered to assess the wound microenvironment *via* pH-responsive fluorescence quenching of EuBG particles and H_2O_2-induced chromatic alterations in MoO_{3-x} nanosheets. This novel method

enabled real-time monitoring of the wound's status, facilitating efficient treatment and recovery. The amalgamation of these materials offers both therapeutic and diagnostic capabilities in wound management. This innovative dressing offers a dual-purpose solution for tracking diabetic wound status and promoting healing.[155] A wearable, flexible red and blue LED (r&bLED) patch was developed, and controllable *via* a mobile system for safe, at-home use. The patch is skin-friendly, flexible and comfortable. A sprayable fibrin gel (F-gel) with

Table 2 Summary of smart theranostic hydrogels for wound management

Hydrogel composite	Monitoring	Bacterial analysis (antibacterial testing)	In vitro biocompatibility (cell lines)	In vivo evaluation (animal model)	Therapeutic effects	Ref.
Diabetic wounds						
MFCPH and PAM	Glucose, pH	E. coli, S. aureus	HUVEC cells	Male SD rats	Antibacterial, wound healing	137
PCHs (AA-AM-AFPBA)	Glucose, pH, temperature		HSF cells	C57BL/6 mice	Antibacterial, wound healing	138
TA-QCMCS/OSA@GOx@AuNC	Glucose	E. coli, S. aureus	L929 cells	Diabetic mouse model	Antibacterial, wound healing	139
GPBT	pH	E. coli, S. aureus, MRSA, MREC	L929 cells	Female SD rats	Antibacterial, antioxidant, anti-inflammatory, hemostatic, angiogenesis	140
PIL-CS	pH	E. coli, S. aureus, Bacillus subtilis, MRSA	L929 cells	Male KM mice	Antibacterial, antioxidant, anti-inflammatory, hemostatic, angiogenesis	141
Bacterial wounds						
BC-AAM₅Ch₂DAC₃	Human activity monitoring	E. coli, S. aureus	293T cells	SD rats (S. aureus)	Antibacterial, wound healing	143
PVA/PANI	Bacterial	E. coli, S. aureus	L929 cells	Rat (S. aureus)	Antibacterial, wound healing	145
PL@Pr-TCPP	pH, bacterial	S. aureus, P. aeruginosa	NIH 3T3 cells	Balb/c mice (S. aureus)	Antibacterial, wound healing	146
GelMA/CMCMAP-GACo	pH	E. coli, MRSA	HUVEC cells, RAW264.7 cells, 3T3 cells	Male C57 mice (MRSA)	Antibacterial, anti-inflammatory, antioxidant, angiogenic	147
PLU@PTc	Bacterial	S. aureus, P. aeruginosa	L929 cells	Female Balb/c mice (S. aureus)	Antibacterial, wound healing	148
PQM	pH	MRSA, P. aeruginosa	NIH-3T3, RAW 264.7 cells	C57BL/6 mice (MRSA)	Antibacterial, wound healing	144
Skin wounds						
PAS/SL@AgNPs	Pressure	S. aureus, E. coli, C. albicans	Mouse fibroblasts	Rat	Antibacterial, Antioxidant, wound healing	151
ALG hydrogel/GO/LVX	pH	S. aureus, P. aeruginosa.			Antibacterial, wound healing	152
DADMAC-PCD/(Gel-DOP)/OSA	Human motion	E. coli, S. aureus	L929 cells	Male Wistar rats	Antibacterial, wound healing	153
Ag@PDA-(CSPBA/CSGA)	Human motion	E. coli, S. aureus	L929 cells	Male SD rats	Antibacterial, antioxidant	154

blue light-sensitive thymoquinone and red light-augmented NADH was presented in this composition. Blue LED light activates thymoquinone to eliminate microbes and biofilms rapidly, while red LED light with NADH boosts mitochondrial function, reducing inflammation, promoting wound healing, and aiding angiogenesis. This innovative technology shows promise for advancing chronic infected wounds.[156] Effective wound care requires efficient drainage and continuous monitoring of wound exudate. This ensures proper healing by preventing infection and maintaining optimal moisture levels. Many recent smart dressings fail to integrate both wound healing and real-time monitoring, limiting their effectiveness. This study presents a smart bandage that combines a biocompatible liquid diode membrane with a highly sensitive 3D PANi mesh (M-PANi) based pH biosensor. The bandage drains wound exudate while continuously monitoring the wound pH. It effectively removes excess exudate and provides real-time updates on wound conditions. The M-PANi sensor has a high sensitivity of 61.5 mV per pH and a wide detection range (pH 4.0 to 10.0), covering both normal and infected wound pH levels. To assess its practicality, tests were conducted on simulated skin and rats, demonstrating the smart bandage's significant potential for clinical use. This smart bandage presents a highly promising solution for both wound exudate management and monitoring, offering an effective approach for advanced and home-based wound care.[157] Jiang et al. designed a flexible bioelectronic system incorporating wirelessly powered, closed-loop sensing and stimulation circuits. This system integrates hydrogel electrodes that enable controlled adhesion and detachment, ensuring adaptable and efficient functionality. In preclinical wound models, the treatment group showed 25% faster healing and 50% improved dermal remodeling compared to controls. Activating pro-regenerative genes in monocytes and macrophages can promote tissue regeneration, neovascularization, and faster dermal recovery. This approach supports the healing process by stimulating key immune cells involved in tissue repair.[158] In 2024, Meng and colleagues presented a multifunctional smart theranostic bandage utilizing conducting polymers. This bandage incorporates pH detection, uric acid (UA) biosensing, and on-demand antibiotic release, employing several conducting polymers to exploit their distinctive intrinsic features.[159] Various theranostic wound dressing materials integrate real-time monitoring with targeted therapies, enhancing healing and personalized care. These smart systems offer innovative solutions for infection control and tissue regeneration.

6. Advancement of hydrogels and artificial intelligence (AI)

The biomedical and pharmaceutical sectors present significant potential for hydrogel applications. Nevertheless, crafting hydrogels with tailored properties for specific uses remains a complex and demanding process. In the development of theranostic hydrogels, it is essential to address both their diagnostic and therapeutic functions. Integrating these dual capabilities into a single hydrogel necessitates meticulous design and thorough experimental testing. AI focuses on creating models and algorithms that enable computers to mimic human cognitive functions. The use of AI and machine learning (ML) algorithms is becoming increasingly crucial in the design and production of innovative, energy-efficient smart technologies.[160,161] The implementation of AI techniques, such as high-throughput experimentation and the integration of results into the database of FDA-approved excipients, has significantly accelerated advancements in biomaterial design and manufacturing.[162] In contrast, leveraging AI-driven algorithms enables the rapid analysis of large datasets, precise prediction of material properties, and insightful recommendations for optimal ingredient selection. Through the use of AI-based optimization techniques, the hydrogel synthesis process can be refined by adjusting factors such as pH, temperature, reaction duration, and swelling characteristics, thereby enhancing both efficiency and performance. Additionally, AI-assisted image analysis and spectroscopic methods play a crucial role in characterizing hydrogel structure, porosity, and mechanical attributes, ultimately improving production quality and ensuring consistency.[163,164]

Recently, researchers have advanced soft computing techniques to analyze complex data and develop models. With the rise of AI-based methods, numerous mathematical tools have emerged, including artificial neural networks (ANNs). ANNs, inspired by the workings of the human brain, are capable of generating, deriving, and discovering new information through learning.[165] Boztepe et al. developed a pH- and temperature sensitive poly(N-isopropyl acrylamide-co-acrylic acid) (poly(NIPAAm-co-AAc)) with poly(ethylene glycol) (PEG) interpenetrating polymer network (IPN) hydrogel. The hydrogel was synthesized via free radical solution polymerization using poly(NIPAAm-co-AAc) microgels and PEG. It showed rapid deswelling in response to changes in pH and temperature. DOX was incorporated, and its release was examined under varying conditions. The release data were modeled using ANNs, least squares support vector machines (LS-SVM), and support vector regression (SVR). The ANN model provided the best prediction of DOX release, demonstrating superior accuracy compared to other models based on statistical metrics such as R, RMSE, MSE, and MAPE.[166] Brahima et al. utilized ANNs to model the nonlinear, multivariable drug delivery behavior of poly(NIPAAm-co-AAc) IPN hydrogel systems. Their ANN model effectively predicted hydrogel drug release behaviors, showing strong alignment between predicted outcomes and actual observations.[167] Another study developed alginate–CS

(ALG-CTN) composite beads via the "drip technique", forming a polyelectrolyte complex through ionic interactions. Characterized by FTIR, TGA, SEM-EDS, and BET, these hydrogels were loaded with resveratrol (RST) for cancer therapy. Encapsulation efficiency and drug release were evaluated against Ca-ALG beads, with release kinetics analyzed at varying pH levels.[168] Traditional methods for optimizing parameters often rely on the operator's prior knowledge and require time-consuming and labor-intensive experimental adjustments. As the variety of biomaterial inks and the complexity of scaffold geometries increase, these conventional approaches may become less effective. To address this challenge, Chen et al. introduced an AI-assisted high-throughput printing-condition screening system (AI-HTPCSS). This system combines a programmable pneumatic extrusion (bio)printer with an AI-driven image analysis algorithm. AI-HTPCSS quickly identifies optimal printing conditions for producing uniform hydrogel scaffolds. The results demonstrated that scaffolds printed under these optimized conditions exhibited strong mechanical properties, good biological performance in vitro, and improved diabetic wound healing in vivo. This innovative system is set to become a valuable tool for optimizing tissue-engineering scaffold manufacturing via 3D (bio)printing.[169] Despite its promising potential, the advancement of AI-powered multifunctional hydrogels is still in its early stages. AI application requires extensive datasets for effective training, validation, and testing. In hydrogel drug delivery systems, having detailed output data on drug release is as crucial as fine-tuning input parameters. A centralized and standardized system for compiling hydrogel drug release data would streamline cross-study comparisons and improve predictive insights. Establishing a standardized protocol for testing and data processing would ensure consistency across research, facilitating more accurate analyses.[170–172] Although AI-driven hydrogel design holds significant promise, further research is essential to fully realize its potential. As technology progresses, AI is expected to play a vital role in advancing innovative hydrogel-based therapies.

7. Clinical applications and regulatory-approved hydrogel dressings

Over 100 hydrogel-based products have received US Food and Drug Administration (FDA) and/or European Medicines Agency (EMA) approval to date, with several more in active clinical trials.[173,174] A meta-analysis of 39 clinical trials ($n = 1786$) reported that hydrogel dressings reduced healing time by ~31 days and achieved >60% improvement in wound closure for chronic wounds.[175] A notable real-world application involves Intrasite™ gel: Fournier et al. documented its use in treating a complex 3 cm facial soft-tissue avulsion from a gunshot wound. With intermittent hydrogel application over eight weeks, the dressing maintained a moist environment, promoted secondary-intention healing, and improved patient comfort compared to conventional gauze dressings.[176] Other

clinically approved systems include Apligraf® and Dermagraft®, which are cellular hydrogel-based therapies approved for diabetic foot and venous leg ulcers.[177] Beyond wound care, hydrogels are increasingly applied in ocular, bone, and soft tissue therapies. Soft contact lenses and ocular delivery systems, among the earliest hydrogel products, highlight their safety and adaptability in sensitive tissues.[173] Additionally, injectable hydrogels for bone regeneration, cartilage repair, and tissue engineering are in clinical trials and early adoption stages, leveraging features like minimally invasive delivery and *in situ* gelation. Soft tissue applications, including wound dressings and implantable scaffolds, are also advancing, supported by robust evidence of biocompatibility and therapeutic efficacy.[178] These developments establish a strong translational foundation, paving the way for next-generation theranostic hydrogel systems that combine sensing, on-demand therapy, and tailored healing responses. While such integrated, multifunctional hydrogels remain largely in pre-clinical development, commercially available products provide proof-of-concept and facilitate the pathway to clinical innovation in smart wound care.

8. Limitations and challenges

Despite significant progress, the clinical translation of theranostic hydrogels remains limited due to several unresolved challenges: (i) Complexity of design and fabrication—multifunctional theranostic hydrogels require the integration of various functional components such as responsive polymers, drug carriers, biosensors, and imaging agents within a single, biocompatible matrix. Achieving this integration without compromising mechanical stability, responsiveness, or biosafety is technically complex and often requires sophisticated synthesis and characterization techniques.[179–182] (ii) Biocompatibility and long-term safety—while many hydrogels are formulated from natural or FDA-approved polymers, the incorporation of nanomaterials (*e.g.*, metal nanoparticles, carbon-based structures) or the use of synthetic chemical crosslinkers can introduce potential toxicity and immunogenicity. Ensuring that all components, including degradation byproducts, are biocompatible remains critical for clinical application. Recent studies have highlighted concerns about immune responses elicited by nanomaterials within hydrogel matrices, particularly regarding excessive oxidative stress, inflammation, or fibrotic encapsulation. Careful evaluation of material composition, degradation pathways, and long-term *in vivo* outcomes is therefore essential to ensure both efficacy and patient safety.[178,183] (iii) Limited real-time sensing accuracy—although progress has been made in embedding sensors for pH, glucose, ROS, or temperature monitoring, the accuracy, stability, and sensitivity of real-time sensing under *in vivo* conditions are still suboptimal. Sensor drift, low signal-to-noise ratios, and challenges in wireless data transmission hinder practical use in clinical settings.[184,185] (iv) Controlled and predictable drug release—while stimuli-responsive hydrogels show great potential for

wound therapy, achieving precise spatiotemporal control over drug release remains challenging. The dynamic nature of wound environments, such as fluctuating pH and variable enzymatic activity, can trigger inconsistent or premature release, potentially compromising therapeutic efficacy or increasing off-target side effects. Swelling-controlled systems are often too slow for rapid wound responses, while stimulus fluctuations can lead to unpredictable kinetics. Multi-layer or burst-control designs may help, but add complexity, and the microenvironmental heterogeneity *in vivo* further impedes consistent performance.[186] (v) Scale-up and regulatory approval—most theranostic hydrogels are still in the pre-clinical or laboratory stage. Scaling up these systems for mass production while maintaining reproducibility and stability is difficult. Additionally, regulatory pathways for multifunctional hybrid devices that combine diagnostics and therapeutics are still evolving and may delay clinical approval.[187] Addressing these limitations will require interdisciplinary collaboration between materials scientists, bioengineers, clinicians, and regulatory bodies. Emphasis should be placed on developing simplified, modular, and clinically adaptable hydrogel platforms that ensure safety, performance, and manufacturability for successful clinical translation.

9. Summary and perspectives

Theranostics, which integrates diagnostic and therapeutic functionalities, is revolutionizing personalized healthcare by enabling precise disease characterization at the molecular level. This approach enables tailored treatment strategies and real-time monitoring, ultimately reducing adverse effects and improving therapeutic outcomes. The application of theranostic hydrogels in this dual-function platform is particularly promising due to their capacity to merge diagnostic tools with therapeutic agents, thus reducing the gap between diagnosis and treatment and improving overall patient care efficiency. Theranostic hydrogels offer significant advantages, including customizable design, excellent biocompatibility, mechanical robustness, and controlled release properties. These characteristics position theranostic hydrogels as promising candidates in the biomedical field. Despite these advantages, several challenges remain. Developing multifunctional hydrogel materials that integrate diagnostic and therapeutic capabilities, ensuring compatibility with medical devices and drugs, and achieving effective clinical outcomes are complex technical hurdles. Selecting appropriate hydrogel materials with sustained drug release and reliable diagnostic capabilities is crucial for their success. Moreover, demanding clinical validation is required to ensure their safety, efficacy, and long-term performance, necessitating extensive human trials that are both time-consuming and costly. Looking ahead, the future development of theranostic hydrogels hinges on several key areas. Firstly, advancements in nanoscale material design will enhance the precision and control of drug delivery systems, enabling more comprehensive diagnostic and therapeutic applications.

Secondly, integrating visual detection technologies, such as fluorescent markers and nanoparticles, will facilitate real-time disease monitoring and support more targeted medical decisions. Thirdly, tailoring hydrogels to the specific genetic and phenotypic profiles of patients will enhance treatment precision and reduce side effects. Additionally, the incorporation of AI in the design and application of theranostic hydrogels is expected to drive innovation, offering new possibilities for personalized medicine. Future theranostic hydrogels are expected to emphasize multifunctionality, controlled drug delivery, real-time monitoring, and advanced nanotechnology integration. They will be designed for personalized treatments, incorporating biomimetic materials to enhance compatibility and therapeutic efficacy. These innovations aim to improve patient outcomes by enabling targeted therapy and responsive healing mechanisms. In conclusion, while still an emerging technology, theranostic hydrogels hold immense potential to revolutionize clinical practice. Continued interdisciplinary collaboration, innovative materials science, and robust clinical validation are essential for overcoming current limitations. As research evolves, these smart hydrogels are poised to become vital tools in the advancement of personalized, responsive, and effective healthcare.

Author contributions

Laxmanan Karthikeyan: writing – review & editing, writing – original draft, conceptualization, validation. Hyun Wook Kang: writing – review & editing, formal analysis, funding acquisition, supervision.

Conflicts of interest

The authors declare there is no conflict of interest.

Abbreviation

10-HDA	10-Hydroxydecanoic acid
3D	Three-dimensional
AA	Asiatic acid
AAPBA	3-Acrylamidophenylboronic acid
Ag NWs	Silver nanowires
AgNPs	Silver nanoparticles
AHA	Aminated hyaluronic acid
AI	Artificial intelligence
AIE	Aggregation-induced emission
ALG	Alginate
ANNs	Artificial neural networks
APS	Ammonium persulfate
AuNCs	Gold nanoclusters
$BaTiO_3$	Barium titanate
BC	Bacterial cellulose
BSA	Bovine serum albumin
BSPs	*Bletilla striata* polysaccharides
$CaCl_2$	Calcium chloride
$CaCO_3$	Calcium carbonate
CAT	Catalase
CEC	*N*-Carboxyethyl chitosan
CLP	Collagen-like protein
CNTs	Carbon nanotubes
COFs	Covalent organic frameworks
CPO	Calcium peroxide
CSL	*Capparis spinosa* L. extract
Cur	Curcumin
CuS NPs	Copper sulfide nanoparticles
Cys	Cysteine
DA	Dopamine
DMM	Dextran methacrylate
DOX	Doxorubicin
ECG	Electrocardiogram
ECM	Extracellular matrix
ePL	*ε*-Polylysine
EVs	Extracellular vesicles
FC	Fungal carboxymethyl chitosan
G	Glycerol
GA	Gallic acid
Ga^{3+}	Gallium ions
GaM	Gallium maltolate
Gel	Gelatin
GelMA	Methacrylated gelatin
GG	Guar gum
GO	Graphene oxide
GOx	Glucose oxidase
GrE	Graviola fruit extract
H_2O_2	Hydrogen peroxide
HA	Hyaluronic acid
HEC	Hydroxyethyl cellulose
IPN	Interpenetrating network
IPS	Instant protection spray
LVX	Levofloxacin
MBA	Methylene bisacrylamide
ML	Machine learning
MOF	Metal–organic framework
MRSA	Multidrug-resistant *Staphylococcus aureus*
NDs	Nanodiamonds
NIPAM	*N*-Isopropylacrylamide
NIR	Near infrared
NO	Nitric oxide
OBSPs	Oxidized *Bletilla striata* polysaccharides
OSA	Oxidized sodium alginate
PA	Poly(thiophene-3-acetic acid)
PAA	Polyacrylic acid
PAM	Polyacrylamide
PANI	Polyaniline
PBNPs	Prussian blue nanoparticles
PBS	Phosphate-buffered saline
PC	Photonic crystal
PCD	Polycyclodextrin
PDA	Polydopamine
PEBSA	Poly(ethylene brassylate-*co*-squaric acid)

PEG	Poly(ethylene glycol)
PET	Polyethylene terephthalate
PF127	Pluronic F127
pH	Potential of hydrogen
PLATMC	Poly(lactic acid-co-trimethylene carbonate)
PNA	Poly(N-isopropylacrylamide-co-allyloxybenzaldehyde)
pNIPAAm	Poly(N-isopropylacrylamide)
POD	Peroxidase
PTA	Photothermal agent
PTA	Poly(thioctic acid)
PTT	Photothermal therapy
PVA	Polyvinyl alcohol
PVP	Poly(vinyl pyrrolidone)
Q	Quercetin
QAC	Quaternary ammonium chitosan
QCMCS	Quaternary carboxymethyl chitosan
QCS	Chitosan quaternary ammonium salt
rGO	Reduced graphene oxide
Rif	Rifampicin
ROS	Reactive oxygen species
SA	Sodium alginate
SDH	Succinate dehydrogenase
SF	Silk fibroin
SIPNs	Semi-interpenetrating polymer networks
SNP	Sodium nitroprusside
SOD	Superoxide dismutase
SVR	Support vector regression
TA	Tannic acid
TP	Polyphenols
UA	Uric acid
UV	Ultraviolet
ZnO NPs	Zinc oxide nanoparticles

Data availability

No primary research results, software, or code have been included and no new data were generated or analyzed as part of this minireview.

Acknowledgements

References

1 S. Kim, Y. H. No, R. Sluyter, K. Konstantinov, Y. H. Kim and J. H. Kim, *Coord. Chem. Rev.*, 2024, **500**, 215530.

2 J. Guo, H. Xiong, H. Liu, T. Zhang and X. Sun, *Coord. Chem. Rev.*, 2023, **497**, 215430.

3 L. Karthikeyan, B. Rithisa, S. Min, H. Hong, H. Kang, R. Thangam and R. Vivek, *Chem. Eng. J.*, 2024, **493**, 152530.

4 K. Charu Nanthini, R. Thangam, L. Karthikeyan, B. Rithisa, P. Abdul Rasheed, S. Min, H. Kang, N. Kannikaparameswari and R. Vivek, *Coord. Chem. Rev.*, 2024, **518**, 216043.

5 M. Puccetti, M. Pariano, A. Schoubben, S. Giovagnoli and M. Ricci, *Pharmacol. Res.*, 2024, **201**, 107086.

6 C. Zheng, W. Li, Y. Shi, S. Wei, K. Liu, J. Cheng, L. Ji and Y. Lu, *Nano Energy*, 2023, **109**, 108245.

7 K. Dong, X. Peng and Z. L. Wang, *Adv. Mater.*, 2020, **32**, 1902549.

8 T. Y. Kim, J. W. Mok, S. H. Hong, S. H. Jeong, H. Choi, S. Shin, C.-K. Joo and S. K. Hahn, *Nat. Commun.*, 2022, **13**, 6801.

9 P. Li, G.-H. Lee, S. Y. Kim, S. Y. Kwon, H.-R. Kim and S. Park, *ACS Nano*, 2021, **15**, 1960–2004.

10 Y. Qin, F. Cui, Y. Lu, P. Yang, W. Gou, Z. Tang, S. Lu, H. S. Zhou, G. Luo, X. Lyu and Q. Zhang, *J. Controlled Release*, 2025, **377**, 354–375.

11 G. Belge Bilgin, C. Bilgin, B. J. Burkett, J. J. Orme, D. S. Childs, M. P. Thorpe, T. R. Halfdanarson, G. B. Johnson, A. T. Kendi and O. Sartor, *Theranostics*, 2024, **14**, 2367–2378.

12 O. Wichterle and D. Lím, *Nature*, 1960, **185**, 117–118.

13 J. Kopecek, *J. Polym. Sci., Part A: Polym. Chem.*, 2009, **47**, 5929–5946.

14 K. Yan, Q. Zhang, Q. Liu, Y. Han and Z. Liu, *Theranostics*, 2025, **15**, 915–942.

15 Y. Zheng, C. Pan, P. Xu and K. Liu, *J. Nanobiotechnol.*, 2024, **22**, 57.

16 P. M. Tehrany, P. Rahmanian, A. Rezaee, G. Ranjbarpazuki, F. Sohrabi Fard, Y. Asadollah salmanpour, M. A. Zandieh, A. Ranjbarpazuki, S. Asghari, N. Javani, N. Nabavi, A. R. Aref, M. Hashemi, M. Rashidi, A. Taheriazam, A. Motahari and K. Hushmandi, *Environ. Res.*, 2023, **238**, 117087.

17 Y. Cao, T. Sun, B. Sun, G. Zhang, J. Liu, B. Liang, C. Zheng and X. Kan, *J. Nanobiotechnol.*, 2023, **21**, 464.

18 M. Tang, J. Song, S. Zhang, X. Shu, S. Liu, M. Ashrafizadeh, Y. N. Ertas, Y. Zhou and M. Lei, *J. Transl. Med.*, 2024, **22**, 970.

19 C. Xu, S. Guan, H. Zhang, W. Fan, X. Zhuang and X. Dong, *J. Mater. Chem. A*, 2025, **13**, 450–459.

20 S. Liu, M. R. Rahman, H. Wu, W. Qin, Y. Wang and G. Su, *J. Mater. Chem. B*, 2025, **13**(4), 1229–1251.

21 Q. Wang, Y. Li, Y. Lin, Y. Sun, C. Bai, H. Guo, T. Fang, G. Hu, Y. Lu and D. Kong, *Nano-Micro Lett.*, 2024, **16**, 87.

22 Z. Li, P. Song, G. Li, Y. Han, X. Ren, L. Bai and J. Su, *Mater. Today Bio*, 2024, **25**, 101014.

23 B. Zhou, X. Jiang, X. Zhou, W. Tan, H. Luo, S. Lei and Y. Yang, *Biomater. Res.*, 2023, **27**, 86.

24 A. Khan, M. Zaman, M. A. Waqar, A. Mahmood, T. Shaheer, R. M. Sarfraz, K. Shahzadi, A. A. Khan, A. M. Alanazi, M. K. Kundu, M. R. Islam, A. Alexiou and M. Papadakis, *BMC Pharmacol. Toxicol.*, 2024, **25**, 31.

25 J. H. Lee, *Biomater. Res.*, 2018, **22**, 27.

26 S. Bashir, M. Hina, J. Iqbal, A. H. Rajpar, M. A. Mujtaba, N. A. Alghamdi, S. Wageh, K. Ramesh and S. Ramesh, *polymers*, 2020, **12**(11), 2702.

27 J. Zhu, H. Han, F. Li, X. Wang, J. Yu, X. Qin and D. Wu, *Chem. Mater.*, 2019, **31**, 4436–4450.

28 C.-H. Cheng, Y.-Y. Tu and J.-C. Lin, *Int. J. Mol. Sci.*, 2022, **23**, 14806.

29 M. Ghahremani-nasab, N. Akbari-Gharalari, A. Rahmani Del Bakhshayesh, A. Ghotaslou, A. Ebrahimi-kalan, M. Mahdipour and A. Mehdipour, *Stem Cell Res. Ther.*, 2023, **14**, 326.

30 N. Asadi, H. Sadeghzadeh, A. Rahmani Del Bakhshayesh, A. Nezami Asl, M. Dadashpour, N. Karimi Hajishoreh, S. Kaamyabi and A. Akbarzadeh, *BMC Biotechnol.*, 2023, **23**, 21.

31 S. Lanzalaco, J. Mingot, J. Torras, C. Alemán and E. Armelin, *Adv. Eng. Mater.*, 2023, **25**, 2201303.

32 C. Lin, T.-W. Lu, F.-Y. Hsu, T.-W. Huang, M.-H. Ho, H.-T. Lu and F.-L. Mi, *Carbohydr. Polym.*, 2025, **351**, 123051.

33 Y. Xie, G. Li, J. Wu, J. Zhu, X. Cai, P. Zhao, D. Zhang and Y. Zhong, *Carbohydr. Polym.*, 2025, **348**, 122864.

34 K. Hemmati, A. Masoumi and M. Ghaemy, *RSC Adv.*, 2015, **5**, 85310–85318.

35 M. Gorbunova, A. Ovcharuk and L. Lemkina, *Int. J. Biol. Macromol.*, 2024, **278**, 134948.

36 J. Zhu, C. Tang, M. Zhang, M. Zhang and L. Fu, *Eur. Polym. J.*, 2024, **207**, 112809.

37 P. M. Kharkar, K. L. Kiick and A. M. Kloxin, *Chem. Soc. Rev.*, 2013, **42**, 7335–7372.

38 K. Ravishankar and R. Dhamodharan, *React. Funct. Polym.*, 2020, **149**, 104517.

39 L. Wang, X. Zhang, K. Yang, Y. V. Fu, T. Xu, S. Li, D. Zhang, L.-N. Wang and C.-S. Lee, *Adv. Funct. Mater.*, 2020, **30**, 1904156.

40 W. Huang, Y. Wang, Z. Huang, X. Wang, L. Chen, Y. Zhang and L. Zhang, *ACS Appl. Mater. Interfaces*, 2018, **10**, 41076–41088.

41 Y. Chan Choi, J. S. Choi, Y. J. Jung and Y. W. Cho, *J. Mater. Chem. B*, 2014, **2**, 201–209.

42 Y. Liang, Z. Li, Y. Huang, R. Yu and B. Guo, *ACS Nano*, 2021, **15**, 7078–7093.

43 K. Laxmanan, I. Yadav, P. K. Barani, M. Meena, H. W. Kang and M. Dhanka, *Mater. Today Commun.*, 2025, **46**, 112936.

44 Y. Yuan, S. Shen and D. Fan, *Biomaterials*, 2021, **276**, 120838.

45 D. Fan, R. Xie, X. Liu, H. Li, Z. Luo, Y. Li, F. Chen and W. Zeng, *J. Mater. Chem. B*, 2024, **12**, 5525–5534.

46 Y. Gao, X. Chen, C. He, Z. Zhang and J. Yu, *Biomater. Sci.*, 2025, **13**, 3192–3212, DOI: **10.1039/D4BM01657B**.

47 C. S. M. Fernandes, A. S. Pina and A. C. A. Roque, *Biomaterials*, 2021, **268**, 120563.

48 N. H. Thang, T. B. Chien and D. X. Cuong, *Gels*, 2023, **9**(7), 523.

49 M. Chelu, J. M. Calderon Moreno, A. M. Musuc and M. Popa, *gels*, 2024, **10**(9), 547.

50 A. Dan, H. Singh, T. K. Shah, W. M. Sheikh, M. Shafi, L. Karthikeyan, J. Jan, S. Hassan, S. M. Bashir and M. Dhanka, *J. Drug Delivery Sci. Technol.*, 2025, **110**, 107075.

51 A. Dan, A. Panigrahi, H. Singh, V. Murali, M. Meena, P. Goyel, L. Karthikeyan, S. K. Misra, N. Varghese, S. S. Babu, Y. B. Dalvi and M. Dhanka, *Biomater. Sci.*, 2025, DOI: **10.1039/D5BM00133A**.

52 Y. Fan, H. Wang, C. Wang, Y. Xing, S. Liu, L. Feng, X. Zhang and J. Chen, *Polymers*, 2024, **16**(19), 2818.

53 H. Dave, H. Vithalani, H. Singh, I. Yadav, A. Jain, A. Pal, N. Patidar, A. Navale and M. Dhanka, *Small*, 2025, **21**, 2405508.

54 T. K. N. Duong, T. T. Truong, T. N. L. Phan, T. X. Nguyen, V. H. M. Doan, T. T. Vo, J. Choi, U. Pal, P. Dhar, B. Lee, J. Oh and S. Mondal, *Aggregate*, 2025, e70047.

55 G. Baishya, B. Parasar, M. Limboo, R. Kumar, A. Dutta, A. Hussain, M. M. Phukan and D. Saikia, *Discover Mater.*, 2024, **4**, 40.

56 L. Huang, Z. Guo, X. Yang, Y. Zhang, Y. Liang, X. Chen, X. Qiu and X. Chen, *Theranostics*, 2025, **15**, 460–493.

57 L. Karthikeyan, P. A. Rasheed, Y. Haldorai and R. Vivek, *ACS Appl. Polym. Mater.*, 2023, **5**, 7167–7179.

58 L. Karthikeyan, V. Yasothamani, Y. Haldorai, J. R. S. Selvan Christyraj and R. Vivek, *ACS Appl. Nano Mater.*, 2023, **6**, 6279–6291.

59 K. Wu, D. Su, J. Liu, R. Saha and J.-P. Wang, *Nanotechnology*, 2019, **30**, 502003.

60 H. Wang, Y. Wu, H. Zou, Z. Song, Y. Wang, H. Wang and M. Zhou, *ACS Appl. Nano Mater.*, 2023, **6**, 4834–4843.

61 L. Karthikeyan, S. Sobhana, V. Yasothamani, K. Gowsalya and R. Vivek, *Biomed. Eng. Adv.*, 2023, **5**, 100082.

62 H. Xin, D. S. A. A. Maruf, F. Akin-Ige and S. Amin, *Emergent Mater.*, 2024, DOI: **10.1007/s42247-024-00930-8**.

63 N. Tang, Y. Zheng, D. Cui and H. Haick, *Adv. Healthcare Mater.*, 2021, **10**, 2101292.

64 K. Youssef, A. Ullah, P. Rezai, A. Hasan and A. Amirfazli, *Mater. Today Bio*, 2023, **22**, 100764.

65 Y.-L. Ji, Y. Zhang, J. Lu, F. Gao, X. Lv, X. Qu, G. Zhu, T. Tian, H. Pang, Y. Tian and X. Dong, *Adv. Healthcare Mater.*, 2025, **14**, 2404723.

66 Z. Xiong, C. Feng, J. Tang, X. Sun, Y. Yang, H. Zhou, T. Wang, X. Wang, S. Liu, P. Lei and W. Liao, *Chem. Eng. J.*, 2025, **513**, 162986.

67 H. Cao, L. Duan, Y. Zhang, J. Cao and K. Zhang, *Signal Transduction Targeted Ther.*, 2021, **6**, 426.

68 J. M. Unagolla and A. C. Jayasuriya, *Appl. Mater. Today*, 2020, **18**, 100479.

69 J. Li, Y. Yang, G. Zhang, J. Sun, Y. Li and B. Song, *Nano Today*, 2025, **60**, 102554.

70 M. Wang, Y. Luo, T. Wang, C. Wan, L. Pan, S. Pan, K. He, A. Neo and X. Chen, *Adv. Mater.*, 2021, **33**, 2003014.

71 T. N. Demidova-Rice, M. R. Hamblin and I. M. Herman, *Advances in Skin & Wound Care*, 2012, vol. 25.

72 Y. Liang, J. He and B. Guo, *ACS Nano*, 2021, **15**, 12687–12722.

73 J. Koehler, F. P. Brandl and A. M. Goepferich, *Eur. Polym. J.*, 2018, **100**, 1–11.

74 S. Guo and L. A. DiPietro, *J. Dent. Res.*, 2010, **89**, 219–229.

75 T. Zhang, Z. Tai, F. Miao, Y. Zhao, W. Wang, Q. Zhu and Z. Chen, *J. Mater. Chem. B*, 2024, **12**, 12338–12348.

76 W. Liang, N. Ni, Y. Huang and C. Lin, *Polymers*, 2023, **15**(21), 4301.

77 L. Karthikeyan, B. Rithisa and R. Vivek, *J. Mater. Chem. B*, 2023, **11**, 9005–9018.

78 Q. Wang, Z. Zhang, J. Yin, L. Shen, L. Zhu, C. Redshaw and Q. Zhang, *Int. J. Biol. Macromol.*, 2025, **288**, 138716.

79 L. Qiao, Y. Liang, J. Chen, Y. Huang, S. A. Alsareii, A. M. Alamri, F. A. Harraz and B. Guo, *Bioact. Mater.*, 2023, **30**, 129–141.

80 J. He, M. Shi, Y. Liang and B. Guo, *Chem. Eng. J.*, 2020, **394**, 124888.

81 C. Zhang, H. Zhao, S. Geng, C. Li, J. Liu, Y. Chen, M. Yi, Y. Liu, F. Guan and M. Yao, *Biomacromolecules*, 2024, **25**, 7750–7766.

82 Z. Li, Y. Huang, J. Luo, J. Chen, S. Huang, X. Zhao and B. Guo, *Chem. Eng. J.*, 2024, **499**, 156381.

83 T. Ma, L. Yan, B. Wang, Q. Gong, G. Wang, T. Chen, S. Liu, H. Wei, G. He, Y. Zhang, L. Fan and Y. Chu, *Eur. Polym. J.*, 2024, **221**, 113527.

84 P. Wang, Z. Hou, Z. Wang and X. Luo, *ACS Appl. Mater. Interfaces*, 2024, **16**, 9656–9668.

85 Y. Cheng, X. Liu, F. Fan, Y. Zhang, M. Cao, L. Bai, H. Ming, H. Chen, Y. Liu, Y. Yu and Y. Wang, *Biomater. Sci.*, 2025, **13**, 758–776.

86 Y. Wang, F. Frascella, C. G. Gaglio, C. F. Pirri, Q. Wei and I. Roppolo, *ACS Appl. Mater. Interfaces*, 2024, **16**, 57778–57791.

87 Y. Ma, J. You, J. Hou, Y. Shi and E. Zhao, *J. Mater. Chem. B*, 2025, **13**, 1326–1337.

88 Z.-H. Xu, P. Sun, X. Zhang, J.-Y. Zhang, Y.-F. Gao, C. Liang, Q.-M. Zhang, W.-W. Gao and Y.-M. Xia, *J. Appl. Polym. Sci.*, 2024, **141**, e55748.

89 K. M. Rao, M. S. Prasad, A. G. Babu, P. Rosaiah, M. R. Karim and S. S. Han, *Int. J. Biol. Macromol.*, 2025, **284**, 137849.

90 D. An, Z. Wang, Y. Ning, Y. Yue, H. Xuan, Y. Hu, M. Yang, H. Zhou, Q. Liu, X. Wang, P. Wang, Z. Zhu, J. Rao and J. Zhang, *ACS Omega*, 2024, **9**, 34413–34427.

91 J. Feng, W. Gao, P. Ge, S. Chang, T. Wang, Q. Zhao, B. He and S. Pan, *ACS Appl. Mater. Interfaces*, 2024, **16**, 65877–65889.

92 J. Xin, Z. Yang, S. Zhang, L. Sun, X. Wang, Y. Tang, Y. Xiao, H. Huang and W. Li, *J. Nanobiotechnol.*, 2024, **22**, 439.

93 J. Zhou, R. Cha, Z. Wu, C. Zhang, Y. He, H. Zhang, K. Liu, M. S. Fareed, Z. Wang, C. Yang, Y. Zhang, W. Yan and K. Wang, *Nano Today*, 2023, **49**, 101801.

94 Q. Wang, X. Liang, L. Shen, H. Xu, Z. Wang, C. Redshaw and Q. Zhang, *Biomacromolecules*, 2024, **25**, 388–399.

95 H. Liu, X. Wei, H. Peng, Y. Yang, Z. Hu, Y. Rao, Z. Wang, J. Dou, X. Huang, Q. Hu, L. Tan, Y. Wang, J. Chen, L. Liu, Y. Yang, J. Wu, S. Hu, S. Lu, W. Shang and X. Rao, *Adv. Mater.*, 2024, **36**, 2412154.

96 Y. Huang, Z. Fu, H. Wang, Z. Liu, M. Gao, Y. Luo, M. Zhang, J. Wang and D. Ni, *Adv. Sci.*, 2024, **11**, 2404813.

97 M. Yu, Y. Guo, S. Zhou, Y. Li, Z. Deng, X. Zhao and Y. Han, *J. Mater. Sci. Technol.*, 2025, **219**, 189–204.

98 P. Zhu, J. Wu, Z. Chang, F. Yang, X. Zhang, K. Hou, D. Ping and S. Li, *Int. J. Biol. Macromol.*, 2025, **289**, 138883.

99 Z. Bei, L. Ye, Q. Tong, Y. Ming, T. Yang, Y. Zhu, L. Zhang, X. Li, H. Deng, J. Liu, W. Chen, B. Chu and Z. Qian, *Cell Rep. Phys. Sci.*, 2024, **5**, 102289.

100 Y. Zhou, H. Huang, Q. Yuan, J. Ren, J. Wu, X. Zhao, Y. Lin, Z. Lin and L. Xu, *Biomater. Adv.*, 2025, **169**, 214143.

101 C. Cheng, X. Pu, X. Peng, Y. Luo, X. Wei, L. Wang, Y. Wang and X. Yu, *Colloids Surf., A*, 2025, **705**, 135672.

102 M. Jallab, M. Ghaheri, B. Javan, V. Erfani-Moghadam, M. Ghaffari and A. Goudarzi, *J. Ind. Eng. Chem.*, 2024, **146**, 441–455.

103 Y. Huang, M. Song, X. Li, Y. Du, Z. Gao, Y.-Q. Zhao, C. Li, H. Yan, X. Mo, C. Wang, G. Hou and X. Xie, *Mater. Today Bio*, 2024, **28**, 101214.

104 P. Choudhary, B. Ramalingam, S. Bose and S. K. Das, *Biomater. Sci.*, 2025, **13**, 639–658.

105 S. Khattak, I. Ullah, M. Sohail, M. U. Akbar, M. A. Rauf, S. Ullah, J. Shen and H.-T. Xu, *Aggregate*, 2025, **6**, e688.

106 X. Liu, Z. Guo, J. Wang, W. Shen, Z. Jia, S. Jia, L. Li, J. Wang, L. Wang, J. Li, Y. Sun, Y. Chen, M. Zhang, J. Bai, L. Wang and X. Li, *Adv. Healthcare Mater.*, 2024, **13**, 2303824.

107 H. Aguayo-Morales, L. E. Cobos-Puc, C. M. Lopez-Badillo, E. Oyervides-Muñoz, G. Ramírez-García and J. A. Claudio-Rizo, *J. Biomed. Mater. Res., Part A*, 2024, **112**, 1760–1777.

108 Y. Wu, Y. Bei, W. Li, W. Lu, J. Zhu, Z. Zhang, T. Zhang, S. Liu, K. Chen, H. Jin, L. Li, M. Li, J. Gao and X. Pan, *Adv. Sci.*, 2024, **11**, 2400898.

109 Q. Guo, T. Yin, W. Huang, R. Nan, T. Xiang and S. Zhou, *Adv. Healthcare Mater.*, 2024, **13**, 2304536.

110 X. Zhou, Y. Shao, S. Zhou, J. Long, L. Jin, X. Shi, L. Zhou, Y. Zhang and D. Fan, *Colloids Surf., B*, 2024, 114488, DOI: **10.1016/j.colsurfb.2024.114488**.

111 X. Li, L. Guan, X. Li, X. Ou, W. Guo, A. V. Zvyagin, W. Qu, B. Yang and Q. Lin, *Chin. Chem. Lett.*, 2024, 110661, DOI: **10.1016/j.cclet.2024.110661**.

112 M. A. D. Chaerani, H. A. Baraja, I. N. D. Putranti, K. E. Reswari and A. Ainurofiq, *Mater. Today Commun.*, 2025, **42**, 111417.

113 D. Britton, D. Almanzar, Y. Xiao, H.-W. Shih, J. Legocki, P. Rabbani and J. K. Montclare, *ACS Appl. Bio Mater.*, 2024, **7**, 5992–6000.

114 J. Wu, T. Meng, X. Zhang, S. Tang, L. Liu, J. Xue, X. Liu, J. Wang, J. Wen, D. Hu and G. Zhang, *Adv. Healthcare Mater.*, 2025, 2404076.

115 M. Farahani and A. Shafiee, *Adv. Healthcare Mater.*, 2021, **10**, 2100477.

116 N. Thirumalaivasan, K. Kanagaraj, S. Nangan, R. Pothu, S. P. Rajendra, P. Karuppiah and R. Boddula, *Polym. Adv. Technol.*, 2025, **36**, e70132.

117 M. Nazemoroaia, F. Bagheri, S. Z. Mirahmadi-Zare, F. Eslami-kaliji and A. Derakhshan, *Int. J. Pharm.*, 2025, **668**, 124976.

118 A. G. F. Shoair, H. A. Sahyon, M. A. E. Shishtawy, A. S. A. Almalki, A. A. Alqarni, F. Althobaiti, M. M. A. H. Shanab and H. A. Khalaf, *ChemistrySelect*, 2024, **9**, e202404438.

119 H. Z. Dawood, C. Ara, Asmatullah, S. Jabeen, A. Islam and Z. H. Ghauri, *Biopolymers*, 2025, **116**, e23633.

120 S. Li, L. Zhi, Q. Chen, W. Zhao and C. Zhao, *Adv. Healthcare Mater.*, 2024, **13**, 2400089.

121 Q. Huang, Y. Hu, Y. Chen, M. Zhou, Y. Zhang, Z. Sun and Z. Chen, *Carbohydr. Polym.*, 2025, **351**, 123136.

122 Y. Yang, Y. Ma, H. Wang, C. Li, C. Li, R. Zhang, S. Zhong, W. He and X. Cui, *Int. J. Biol. Macromol.*, 2024, **280**, 135939.

123 L. Tang, B. Wang, S. Bai, B. Fan, Z. Zhang, L. Zhang and F. Wang, *Int. J. Biol. Macromol.*, 2024, **281**, 136541.

124 C. Liu, S. Yue, R. Li, L. Wang, K. Zhang, S. Wang, S. Yu, F. Shafiq, Y. Liu and W. Qiao, *Eur. Polym. J.*, 2024, **221**, 113521.

125 S. Qin, H. Li, X. Liu, X. Zheng, X. Zhao, S. Wen, Y. Wang, J. Wen and D. Sun, *Colloids Surf., B*, 2025, **245**, 114345.

126 Z. Lan, L. Guo, A. Fletcher, N. Ang, C. Whitfield-Cargile, L. Bryan, S. Welch, L. Richardson and E. Cosgriff-Hernandez, *Bioact. Mater.*, 2024, **42**, 433–448.

127 K. Wang, W. Li, J. Wu, Z. Yan and H. Li, *Int. J. Biol. Macromol.*, 2024, **279**, 135303.

128 H. Liu, Y. Yang, L. Deng, Z. Shen, Q. Huang, N. G. Shah, W. Chen, Y. Zhang, X. Wang, L. Yu and Z. Chen, *Int. J. Biol. Macromol.*, 2024, **279**, 135177.

129 Y. Wang, M. Zhu, X. Hou, J. He, J. Zhang, H. Qi, M. Xu and X. Wang, *ACS Appl. Nano Mater.*, 2024, **7**, 15128–15142.

130 M. Wei, H. Wang, J. Wu, D. Yang, K. Li, X. Liu, M. Wang, B. Lin and Z. Wang, *ACS Appl. Mater. Interfaces*, 2024, **16**, 21472–21485.

131 C. Huang, L. Dong, B. Zhao, S. Huang, Y. Lu, X. Zhang, X. Hu, Y. Huang, W. He, Y. Xu, W. Qian and G. Luo, *J. Nanobiotechnol.*, 2023, **21**, 387.

132 W. Zhang, S. Zhao, Q. Guan, P. Li and Y. Fan, *ACS Appl. Mater. Interfaces*, 2024, **16**, 8238–8249.

133 X. An, L. Gao, J. Guo, F. Meng, H. Lian, S. Zhang, J. L. Pathak, Y. Li and S. Zhang, *J. Mater. Chem. C*, 2025, **13**, 1999–2009.

134 X. Yi, J. He, X. Wei, H. Li, X. Liu and F. Cheng, *Cellulose*, 2023, **30**, 6523–6538.

135 A. Chhillar and A. Jaiswal, *Adv. Healthcare Mater.*, 2025, **14**, 2404255.

136 S. Szunerits and R. Boukherroub, *Adv. NanoBiomed Res.*, 2024, **4**, 2400040.

137 X. Gong, J. Yang, Y. Zheng, S. Chen, H. Duan, J. Gao, H. Haick, C. Yi and L. Jiang, *Adv. Funct. Mater.*, 2024, **34**, 2315564.

138 X. Yang, L. Chai, Z. Huang, B. Zhu, H. Liu, Z. Shi, Y. Wu, L. Guo, L. Xue and Y. Lei, *J. Nanobiotechnol.*, 2024, **22**, 618.

139 Z. Yang, J. Zhang, C. Wang, F. Yu, W. Yu and Z. Zhao, *Biomater. Sci.*, 2025, **13**, 275–286.

140 H. Zhang, W.-X. Li, S. Tang, Y. Chen, L.-M. Lan, S. Li, M. Xiong, X. Hu, Y.-H. Liu, J. Sun and G.-B. Jiang, *Adv. Funct. Mater.*, 2023, **33**, 2305580.

141 Y. Zong, B. Zong, R. Zha, Y. Zhang, X. Li, Y. Wang, H. Fang, W.-L. Wong and C. Li, *Adv. Healthcare Mater.*, 2023, **12**, 2300431.

142 X. Sun, C. Ding, M. Qin and J. Li, *Small*, 2024, **20**, 2306960.

143 C. Yang, H. Feng, X. Liu, Y. Guo, M. Sun, W. Wang, Q. Kang, Z. Su, W. Zhu, H. Wang and L. Xiao, *Chem. Eng. J.*, 2024, **498**, 155295.

144 W. Zou, Y. Zhou, S. Zhong, F. Liao, J. Lu, L. Zhang and D. Sun, *Chem. Eng. J.*, 2024, **497**, 154945.

145 X. Zhang, S. Zhang, X. Chen, Z. Ye, W. Liu, X. Liu and X. Wang, *Int. J. Biol. Macromol.*, 2024, **269**, 132080.

146 P. Ran, T. Xia, H. Zheng, F. Lei, Z. Zhang, J. Wei and X. Li, *Acta Biomater.*, 2023, **155**, 292–303.

147 D. Deng, L. Liang, K. Su, H. Gu, X. Wang, Y. Wang, X. Shang, W. Huang, H. Chen, X. Wu, W.-L. Wong, D. Li, K. Zhang, P. Wu and K. Wu, *Nano Today*, 2025, **60**, 102559.

148 P. Ran, H. Zheng, W. Cao, X. Jia, G. Zhang, Y. Liu and X. Li, *ACS Appl. Mater. Interfaces*, 2022, **14**, 49375–49388.

149 Y. Gao, Z. Qiu, L. Liu, M. Li, B. Xu, D. Yu, D. Qi and J. Wu, *J. Polym. Sci.*, 2022, **60**, 2191–2212.

150 A. A. Arafa, O. A. Hakeim, A. A. Nada, M. K. Zahran, N. M. Shaffie and A. Y. Ibrahim, *Int. J. Biol. Macromol.*, 2025, **286**, 138339.

151 Z. Jin, H. Gong, B. Chen, Y. Jiang, Y. Su, J. Zhou, H. Wang and Y. Li, *Int. J. Biol. Macromol.*, 2025, **291**, 138853.

152 P. Punnoy, T. Siripongpreda, C. S. Henry, N. Rodthongkum and P. Potiyaraj, *Int. J. Pharm.*, 2024, **661**, 124406.

153 S. Vakili, Z. Mohamadnia and E. Ahmadi, *Biomacromolecules*, 2024, **25**, 7704–7722.

154 W. Shi, H. Li, C. Xu, G. Wu, J. Chen, J. Zhang, L. Liang, Q. Wu, Y. Liang, G. Li and W. Tang, *npj Flexible Electron.*, 2024, **8**, 82.

155 J. Huang, J. Huang, X. Zhang, Q. Xie, Y. Zheng, C. Shu, Z. Shi, X. Wang, J. Chen, B. Ma, C. Wu and Y. Zhu, *Mater. Horiz.*, 2025, **12**, 267–283.

156 M. Li, C. Wang, Q. Yu, H. Chen, Y. Ma, L. Wei, M. X. Wu, M. Yao and M. Lu, *Nat. Commun.*, 2024, **15**, 9380.

157 X. Wang, J. Cheng and H. Wang, *Microsyst. Nanoeng.*, 2024, **10**, 193.

158 Y. Jiang, A. A. Trotsyuk, S. Niu, D. Henn, K. Chen, C.-C. Shih, M. R. Larson, A. M. Mermin-Bunnell, S. Mittal, J.-C. Lai, A. Saberi, E. Beard, S. Jing, D. Zhong, S. R. Steele, K. Sun, T. Jain, E. Zhao, C. R. Neimeth, W. G. Viana, J. Tang, D. Sivaraj, J. Padmanabhan, M. Rodrigues, D. P. Perrault, A. Chattopadhyay, Z. N. Maan, M. C. Leeolou, C. A. Bonham, S. H. Kwon, H. C. Kussie, K. S. Fischer, G. Gurusankar, K. Liang, K. Zhang, R. Nag, M. P. Snyder, M. Januszyk, G. C. Gurtner and Z. Bao, *Nat. Biotechnol.*, 2023, **41**, 652–662.

159 L. Meng, S. Liu, B. A. Borsa, M. Eriksson and W. C. Mak, *Commun. Mater.*, 2024, **5**, 28.

160 K. Sagdic, I. Eş, M. Sitti and F. Inci, *Trends Biotechnol.*, 2022, **40**, 987–1003.

161 C. Wang, E. Shirzaei Sani and W. Gao, *Adv. Funct. Mater.*, 2022, **32**, 2111022.

162 D. Reker, Y. Rybakova, A. R. Kirtane, R. Cao, J. W. Yang, N. Navamajiti, A. Gardner, R. M. Zhang, T. Esfandiary, J. L'Heureux, T. von Erlach, E. M. Smekalova, D. Leboeuf, K. Hess, A. Lopes, J. Rogner, J. Collins, S. M. Tamang, K. Ishida, P. Chamberlain, D. Yun, A. Lytton-Jean, C. K. Soule, J. H. Cheah, A. M. Hayward, R. Langer and G. Traverso, *Nat. Nanotechnol.*, 2021, **16**, 725–733.

163 X. Shen, J. Du, J. Sun, J. Guo, X. Hu and C. Wang, *ACS Appl. Mater. Interfaces*, 2020, **12**, 39639–39648.

164 T. A. Saleh, G. Fadillah and E. Ciptawati, *J. Polym. Res.*, 2021, **28**, 197.

165 H. Demir, B. Arica-Yegin and L. Oner, *J. Drug Delivery Sci. Technol.*, 2018, **47**, 215–222.

166 C. Boztepe, A. Künkül and M. Yüceer, *J. Drug Delivery Sci. Technol.*, 2020, **57**, 101603.

167 S. Brahima, C. Boztepe, A. Kunkul and M. Yuceer, *Mater. Sci. Eng., C*, 2017, **75**, 425–432.

168 A. B. Nazlı and Y. S. Açıkel, *J. Drug Delivery Sci. Technol.*, 2019, **53**, 101199.

169 B. Chen, J. Dong, M. Ruelas, X. Ye, J. He, R. Yao, Y. Fu, Y. Liu, J. Hu, T. Wu, C. Zhou, Y. Li, L. Huang, Y. S. Zhang and J. Zhou, *Adv. Funct. Mater.*, 2022, **32**, 2201843.

170 M. Vigata, C. Meinert, D. W. Hutmacher and N. Bock, *Pharmaceutics*, 2020, **12**, 1188.

171 A. S. Vasilevich, A. Carlier, J. de Boer and S. Singh, *Trends Biotechnol.*, 2017, **35**, 743–755.

172 C. Owh, V. Ow, Q. Lin, J. H. M. Wong, D. Ho, X. J. Loh and K. Xue, *Biomater. Adv.*, 2022, **141**, 213100.

173 J. R. Clegg, K. Adebowale, Z. Zhao and S. Mitragotri, *Bioeng. Transl. Med.*, 2024, **9**, e10680.

174 A. Mandal, J. R. Clegg, A. C. Anselmo and S. Mitragotri, *Bioeng. Transl. Med.*, 2020, **5**, e10158.

175 S. A. Hosseini, S. Noruzi, P. Kesharwani and A. Sahebkar, *Int. J. Biol. Macromol.*, 2025, **308**, 142322.

176 M. Y. Fournier, C. K. Cutbirth, D. N. Lam, J. M. Marchena and C. B. Pearl, *Craniomaxillofacial Res. Innov.*, 2022, **7**, 27528464221115228.

177 A. D. Sharma, E. H. Jarman and P. M. Fox, *Plast. Reconstr. Surg. Glob. Open*, 2023, **11**, e4984.

178 P. Lu, D. Ruan, M. Huang, M. Tian, K. Zhu, Z. Gan and Z. Xiao, *Signal Transduction Targeted Ther.*, 2024, **9**, 166.

179 R. Acharya, S. D. Dutta, H. Mallik, T. V. Patil, K. Ganguly, A. Randhawa, H. Kim, J. Lee, H. Park, C. Mo and K.-T. Lim, *J. Nanobiotechnol.*, 2025, **23**, 233.

180 I. S. Protsak and Y. M. Morozov, *Gels*, 2025, **11**, 30.

181 S. J. Patil, V. M. Thorat, A. A. Koparde, R. R. Bhosale, S. D. Bhinge, D. D. Chavan and D. D. Tiwari, *Cureus*, 2024, **16**, e71694.

182 U. S. K. Madduma-Bandarage and S. V. Madihally, *J. Appl. Polym. Sci.*, 2021, **138**, 50376.

183 A. Yadav, D. S. Waghmare, A. Ahir and A. Srivastava, *Regener. Eng. Transl. Med.*, 2025, **11**, 351–378.

184 J. Lan, Y. Gong, B. Lin, A. Xu and R. Liu, *Microchem. J.*, 2024, **205**, 111272.

185 Z. Xu, Y. Hao, A. Luo and Y. Jiang, *Med-X*, 2024, **2**, 24.

186 J. Li and D. J. Mooney, *Nat. Rev. Mater.*, 2016, **1**, 16071.

187 M. C. Catoira, J. González-Payo, L. Fusaro, M. Ramella and F. Boccafoschi, *J. Mater. Sci.: Mater. Med.*, 2020, **31**, 64.